# Cholinergic neurotransmission in different subregions of the substantia nigra differentially controls dopaminergic neuronal excitability and locomotion

by

Jasem Estakhr

M.Sc., Shahid Beheshti University, 2008

A Thesis Submitted in Partial Fulfillment

of the Requirements for the Degree of

**MASTER OF SCIENCE**

in the Department of Biology



University of Victoria

**Supervisory Committee**

Cholinergic neurotransmission in different subregions of the substantia nigra differentially controls dopaminergic neuronal excitability and locomotion

by

Jasem Estakhr

M.Sc., Shahid Beheshti University, 2008

**Supervisory Committee**

Dr. Raad Nashmi, Department of Biology

**Supervisor**

Dr. Brian Christie, Division of Medical Sciences

**Outside Member**

# Abstract

Midbrain dopamine (DA) neurons play a key role in a wide range of behaviours, from motor control, motivation, reward and reinforcement learning. Disorders of midbrain dopaminergic signaling is involved in a variety of nervous system disorders including Parkinson's disease, schizophrenia and drug addiction. Understanding the basis of how dopaminergic neuronal activity in the substantia nigra pars compacta (SNc) governs movements, requires a deep appreciation of how afferent inputs of various neurotransmitter systems create a neuronal circuit that precisely modulates DA neuronal excitability. Two brainstem cholinergic neuclei, the laterodorsal tegmental nucleus (LDT) and the pedunculopontine tegmental nucleus (PPT), have major cholinergic projections to the SNc, despite the fact that the precise mechanisms of cholinergic modulation of DA neuronal activity mediated by nAChRs remain unclear. To dissect out the modulatory roles of the cholinergic system in regulating DAergic neuronal activity in the SNc and locomotion, we employed optogenetics along with electrophysiological and behavioural approaches. My results from whole-cell recordings from lateral and medial SNc DA neurons revealed that lateral DA neurons received predominantly excitatory nAChR mediated cholinergic neurotransmission (monosynaptic nicotinic or disynaptic glutamatergic responses) resulting in greater excitability of DA neurons both at 5 and 15 Hz blue LED light stimulation of cholinergic terminals. However, medial SNc DA neurons received predominantly biphasic current responses that were both inhibitory GABAergic and excitatory nAChR mediated cholinergic neurotransmission. This led to a

net inhibition of action potential firing of DA neurons at 5 Hz blue LED light stimulation of cholinergic terminals, while at 15 Hz stimulation there was an initial inhibition followed by a significant increase of the baseline action potential firing frequency. Furthermore, *in vivo* optogenetic experiments showed that activation of the cholinergic system in the medial SNc resulted in decreased locomotion, while for the lateral SNc led to increased locomotion. Together our findings provide new insights into the role of the cholinergic system in modulating DA neurons in the SNc. The cholinergic inputs to different subregions of the SNc may regulate the excitability of the DA neurons differentially within a tight range from excitation to inhibition which may translate into different kinds of locomotor behaviour.

# Table of Contents

# List of Figures

# List of Tables

# List of Abbreviations

| | |
|---|---|
| **ACh** | Acetylcholine |
| **AChRs** | ACh receptors |
| **AMPA** | α-amino-3-hydroxy-5-methyl-4-isoxazolepropoionic acid |
| **AP amplitude** | Action potential amplitude |
| **AP freq** | Action potential frequency |
| **AP half width** | Action potential half width |
| **BF** | Basal forebrain |
| **BG** | Basal ganglia |
| **ChAT** | Choline acetyltransferase |
| **ChR2** | Channelrhodopsin |
| **CNS** | Central nervous system |
| **CNQX** | 6-cyano-7-nitroquinoxaline-2,3-dione |
| **DA** | Dopamine |
| **DHβE** | Dihydro-β-erythrodine |
| **DNQX** | 6,7-dinitroquinoxaline-2,3-dione |
| **eEPSCs** | Evoked excitatory postsynaptic currents |
| **eIPSCs** | Evoked inhibitory postsynaptic currents |
| **GABA** | Gamma aminobutyric acid |
| **GPe** | Globus pallidus externa |
| **GPi** | Globuls pallidus interna |
| **GPCR** | G-protein coupled receptor |
| **Ih** | Hyperpolarization-activated inward current |
| **KO** | Knockout |
| **LDT** | Laterodorsal tegmental nucleus |
| **mAChRs** | Muscarinic acetylcholine receptors |
| **MED** | Medioventral medulla |
| **MLA** | Methyllycaconitine |
| **MSNs** | Medium spiny neurons |
| **nAChR** | Nicotinic acetylcholine receptor |
| **NAcc** | Nucleus accumbens |
| **NMDA** | N-methyl-D-aspartate receptor |
| **NMDG** | N-methyl--glucamine |
| **PD** | Parkinson disease |
| **PPT** | Pedunculopontine tegmental nucleus |
| **R input** | Input resitance |
| **SN** | Substantia nigra |
| **SNc** | Substantia nigra pars compacta |
| **SNr** | Sbstantia nigra pars reticulata |
| **STN** | Subthalamic  nucleus |
| **TH** | Tyrosine hydroxylase |
| **VAChT** | Vesicular acetylcholine transporter |

| | |
|---|---|
| **VGAT** | Vesicular GABA transporter |
| **V rest** | Resting membrane potential |
| **VTA** | Ventral tegmental area |
| **WT** | Wild type |
| ***(e.g. α4* nAChR)** | Containing (i.e. may contain other nAChR subunits in addition to α4) |

# Acknowledgments

Where do I begin? It is difficult for me to express my emotions, as words are not adequate enough to express what I desire. However, for this purpose I shall try my best.

First of all I would like to thank my supervisor Dr. Raad Nashmi. The completion of this study could not have been possible without his valuable guidance and assistance. The words can not express my gratitude for his kindness, indispensable support, patience, and advice during these years.

I am also indebted to Dr. Kerry Delaney, who expertly gave me advice for experimental design and project development through my graduate education. My appreciation also extends to my thesis committee members, Dr. Brian Christie, Dr. Craig Brown, and Dr. Patrick Nahirney for providing countless advice for my thesis. Thanks also goes to Dr. J. Michael McIntosh from University of Utah for providing us with some useful nicotinic receptors antagonists.

Secondly, my deepest gratitude goes to my wife, Danya, whose tremendous support and understanding pushed me forward everyday. I am also thankful to all my family and other loved ones.

Finally and importantly, my appreciation goes to my laboratory colleagues, Pragya Komal, Kaitlyn Frisby, all the members of the Delaney lab and all my colleagues and friends who helped to sustain a positive attitude in which to do science.

# Dedication

I would like to dedicate this thesis to my amazing wife, Danya, for all her love and support.

To all my family and other loved ones.

To all children around the world who have suffered from war and hunger.

# Chapter 1- Introduction

## 1.1 Overview and rationale

Midbrain dopamine (DA) neurons play a key role in a wide range of behaviours, from motor control, motivation, reward and reinforcement learning (Grace et al., 2007; Howe and Dombeck, 2016; Maskos et al., 2005). Disorders of midbrain dopaminergic signaling leads to a variety of nervous system disorders including Parkinson's disease (PD), schizophrenia and drug addiction. As an intergral component of the basal ganglia, DA neurons of the substantia nigra pars compacta (SNc) are key neural substrates for initiating voluntary movement. The activity of SNc neurons are modulated by several neurotransmitter systems including γ-aminobutyric acid (GABA), glutamate and acetylcholine (ACh) (Nashmi et al., 2007; Xiao et al., 2009, 2015, 2016). The major cholinergic input into the SNc are from two brainstem nuclei: the pedunculopontine tegmental nucleus (PPT) and the laterodorsal tegmental nucleus (LDT) (Clark et al., 2007; Cornwall et al., 1990). ACh released from these nuclei can activate two major classes of ACh receptors on DA neurons, muscarinic and nicotinic acetylcholine receptors (nAChRs)(Foster et al., 2014; Wooltorton et al., 2003). nAChRs play a major role in the facilitation of neurotransmitter release in the central nervous system (CNS). It has been shown that SNc DA neurons contain one of the highest expression of nAChRs in the brain and are powerfully excited by nicotine (Nashmi et al., 2007). However, the detailed modulation of DA neuronal excitability and neurotransmitter release induced from endogenous ACh release from the PPT and LDT onto midbrain DA neurons have not been investigated in detail. Evidence from others have indicated that there may be a

heterogeneity of DA neurons expressed in the SNc (Henny et al., 2012). If this is the case, is this DA neuronal heterogeneity mapped to different regions of the SNc? Furthermore, do these heterogeneous subpopulations of DA SNc neurons mediate different cholinergic mediated responses? Cholinergic neurons of the PPT and LDT both innervate the substantia nigra (SN) in addition to the ventral tegmental area (VTA) (Clarke et al., 1987; Cornwall et al., 1990; Dautan et al., 2016a). Both of these nuclei are actually quite heterogeneous in so far as neurotransmitter makeup. These two nuclei are composed of not only cholinergic but also glutamatergic and GABAergic neurons (Wang and Morales, 2009a). Previous studies have shown that there are two populations of neurons in the PPT whose activity responds differentially to movement (Matsumura et al., 1997; Norton et al., 2011). There were PPT neurons whose action potential firing was positively correlated to movement, while there were also other PPT neurons with neuronal activity negatively correlated to movement (Matsumura et al., 1997; Norton et al., 2011). How can a cholinergic nucleus such as the PPT mediate a seemingly paradoxical effect of both stimulation or inhibition of locomotor activity?

In this study I investigated whether stimulation of cholinergic terminals in two distinct regions of the SNc – the lateral and medial portions, may mediate different cholinergic neurotransmission modalities that would differ in modulating DA neuronal excitability. I also investigated how cholinergic neurotransmission in the medial and lateral SNc modifies locomotor behaviour.

## 1.2 Research objective and hypotheses

The main objective of this study is to provide answers to the following questions: 1) how

does the cholinergic system influence SNc dopaminergic neuronal activity? 2) how does activation of the cholinergic system affects mouse locomotor behaviours?

Identification of the cholinergic afferents in the SNc and the study of their physiological attributes is highly complex and their study by conventional methods is limited. An additional level of complexity in understanding cholinergic modulation of SN function stems from the fact that ACh not only binds to nAChRs on somatodendritic regions of DA neurons, but also activates presynaptic nAChRs, which may facilitate the release of a variety of different neurotransmitters, including GABA and glutamate. Therefore, the primary **hypothesis** that I will test is that endogenous release of ACh modulates SNc activity differentially depending on presynaptic or postsynaptic activation of nAChRs in SNc. Secondly, I **hypothesize** that DA neurons in distinct regions of the SNc, medial SNc and lateral SNc, will be modulated differentially by cholinergic inputs. Finally, I **hypothesize** that medial and lateral SNc DA neurons will have distinct effects in mediating locomotion due to differential cholinergic mediated neurotransmission in these regions.

## 1.3 Background information

### 1.3.1 Basal ganglia and substantia nigra

The basal ganglia (BG) are comprised of a number of subcortical nuclei that communicate with the cerebral cortex to regulate motor behaviour, motivation, reward, and reinforcement (Kreitzer and Malenka, 2008). The key components of the BG are the substantia nigra, dorsal and ventral striatum, ventral pallidum, globus pallidus and

subthalamic nucleus (STN) (Rothwell, 2011). The BG have a bidirectional interaction with the cereberal cortex, thalamus and brainstem to have fine control over locomotor behaviour (Roseberry et al., 2016). The striatum has two kinds of GABAergic medium spiny neurons (MSNs), that have antagonistic effects on downstream structures (Calabresi et al., 2014; Donahue and Kreitzer, 2015; Kreitzer and Malenka, 2008). These neurons are the origin of direct and indirect pathways in the BG. The striatal MSNs expressing DA receptor 1 (D1) are part of the direct pathway and have a key role in locomotor activation and movements (Calabresi et al., 2014; Donahue and Kreitzer, 2015; Kreitzer and Malenka, 2008). In this pathway, release of glutamate from cortical input into dorsal striatum activates D1 MSNs projecting to the substantia nigra pars reticulata (SNr) and globuls pallidus interna (GPi) and cause inhibition of GABAergic neurons in these regions. Consequently, this results in a disinhibition of glutamatergic neurons in the thalamus, which facilitates locomotor behaviour (Figure 1.1) (Calabresi et al., 2014). In addition, DA release from SNc dopaminergic projecting neurons in the dorsal striatum has a key role in facilitating movements. Conversely, striatal MSNs expressing DA receptor 2 (D2) are part of the indirect pathway and are proposed to have a major role in inhibition of movements (Calabresi et al., 2014; Donahue and Kreitzer, 2015; Kreitzer and Malenka, 2008). In the indirect pathway, D2 MSNs project indirectly to SNr through globus pallidus externa (GPe) and the STN. Activation of D2-containing MSNs inhibits GPe GABAergic neurons, which in turn disinhibits STN glutamatergic neurons. The greater the discharge of STN neurons, the greater the activation of SNr GABAergic neurons which in turn inhibits thalamic glutamatergic neurons projecting to

the motor cortex and ultimately results in less locomotor activity (Figure 1.1) (Calabresi et al., 2014).

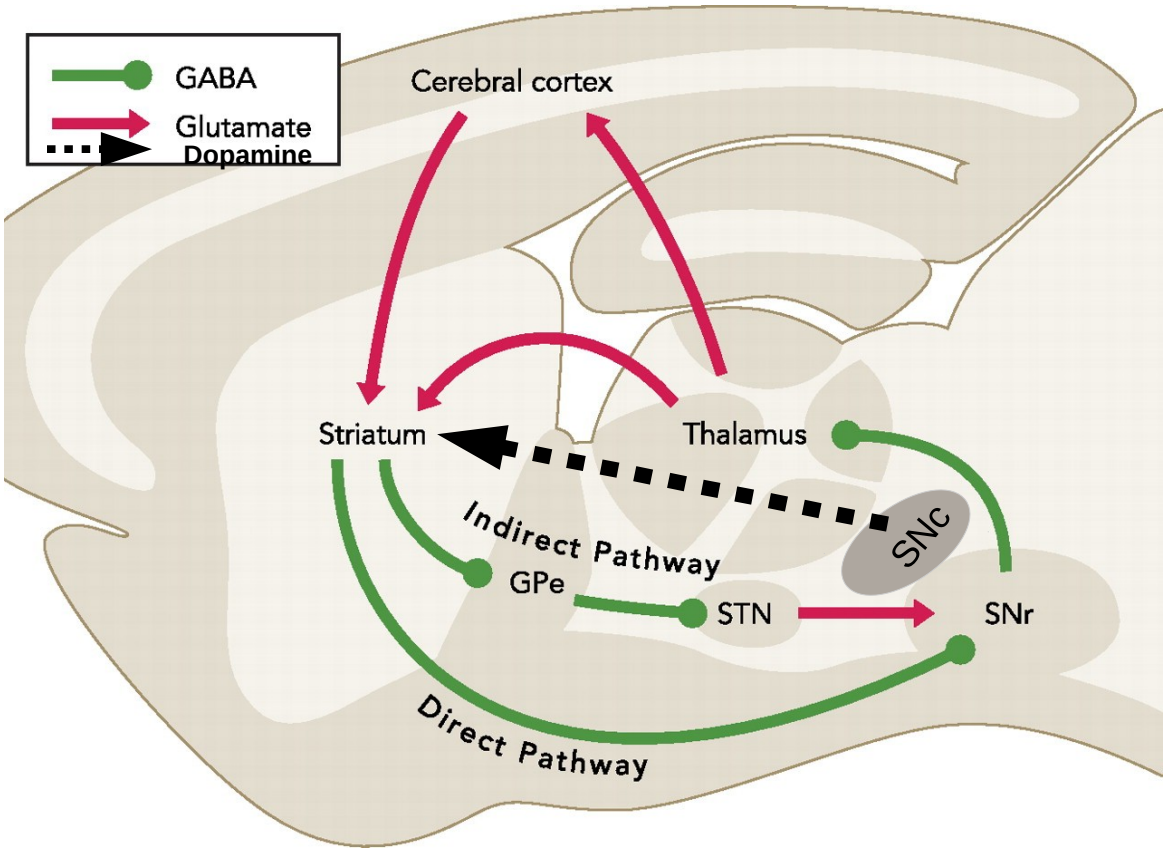


**Figure 1.1** Schematic representation of the direct and indirect pathways in the BG. Activation of the direct pathway leads to facilitation of locomotor behaviour, while activation of indirect pathway results in inhibition of locomotion. SNr: substantia nigra pars reticulata, SNc: substantia nigra pare compacta, GPe: globus pallidus external, STN: sub-thalamic nucleus. Adapted and modified from Kravitz and Kreitzer, 2012.

The SN is a nucleus in the midbrain considered as one of the key components of

the BG. It is made up of two anatomically and functionally distinct portions: the SNc and the SNr. While the SNc is populated mainly by DA neurons, the SNr consists predominantly of GABAergic neurons. These two structures are important for a variety of brain functions, including voluntary movement. SNc DA neurons mainly project to the input structure of the BG, namely the dorsal striatum, and release DA, which regulates MSNs neuronal activity (Calabresi et al., 2014). Motor stimulation and striatonigral activation inhibits GABAergic neuronal activity in the SNr, leading to disinhibition of their target nuclei in the thalamus and brain stem and consequently facilitates movements (Deniau et al., 2007). *In vitro* electrophysiological studies have shown that DA neurons have slow regular firing action potentials (<10 Hz) with long durations of action potential half-widths (>2 ms) (Blythe et al., 2009; Roeper, 2013). In addition, during whole-cell recordings they exhibit a strong hyperpolarization-activated inward current (Ih) (Ungless and Grace, 2012). On the contrary, GABAergic neurons in SNr have higher firing rates (>10 Hz) and short durations of action potentials (<2 ms) (Borgkvist et al., 2015). DA neurons *in vivo* exhibit two types of patterned firing activity: (1) a tonic mode of regularly spaced action potentials that is driven by an intrinsic pacemaker potential or (2) a phasic or burst mode of firing, which depends on the activity of afferent inputs into the SNc (Blythe et al., 2009; Grace and Bunney, 1984a, 1984b; Roeper, 2013)

In Parkinson's disease (PD) the major neuronal deficit comprises a loss of DA neurons in the SNc that results in striatal DA deficiency (Perez, 2015). PD is characterized by hypokinesia, tremor, muscle rigidity, bradykinesia, and postural instability (Jankovic, 2008). It is believed that DA loss induces abnormal bursting

activity in the basal ganglia output nuclei (SNr) due to hypoactivity of direct pathway and hyperactivity of indirect pathway (Mallet et al., 2006), leading to pathological inhibitory tone onto the thalamocortical circuit that disrupts motor planning and execution in PD (Borgkvist et al., 2015; Maurice et al., 2015).

### 1.3.2 Cholinergic system and nicotinic acetylcholine receptors

There are two main sources of ACh in the mammalian brain -- cholinergic projection neurons and cholinergic local interneurons. Cholinergic projection neurons are located in different nuclei throughout the brain, such as the LDT, PPT, the basal forebrain (BF) including the medial septum, and the medial habenula (Figure 1.2A) (Picciotto et al., 2012). Cholinergic interneurons are found in the striatum, nucleus accumbens (NAcc), and neocortex (Figure 1.2) (Dautan et al., 2016a; von Engelhardt et al., 2007). Recently a population of neurons in the globus pallidus and nucleus basalis have been identified that release both ACh and GABA (Saunders et al., 2015b). The cholinergic system, by releasing ACh, plays a major role in the modulation of neuronal activity in many brain regions. In the mammalian brain, ACh, acts as a fast neurotransmitter that can perform a wide range of functions including the control of neuronal excitability, facilitating presynaptic neurotransmitter release, and synchronizing the firing of a group of neurons (Kawai et al., 2007; Mansvelder and McGehee, 2000; Mansvelder et al., 2002; Picciotto et al., 2012; Wonnacott et al., 2006).

**A**

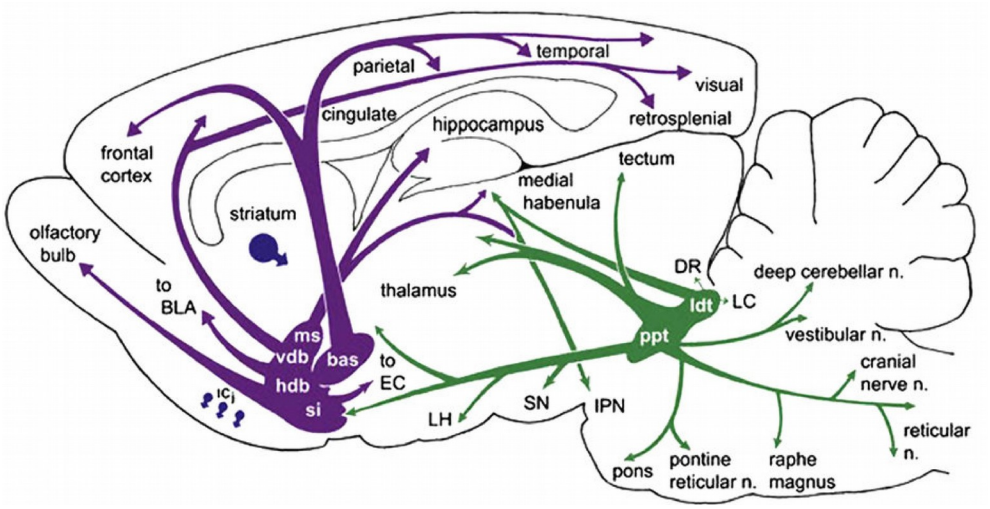


**B**

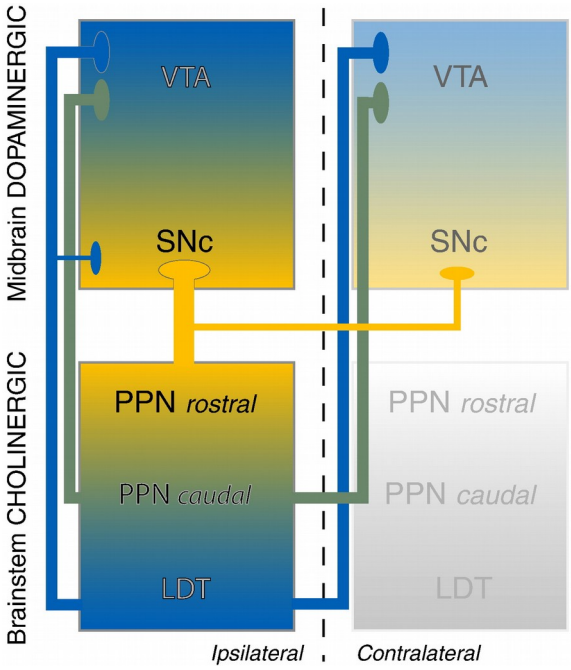


**Figure 1.2 (A)** Schematic representation of the cholinergic system in the rodent brain. Purple: basal forebrain cholinergic system; green: brainstem cholinergic system; blue: cholinergic interneurons. Adapted from Perez-Lloret and Barrantes (2016). BLA: basolateral amygdaloid area, DR: dorsal raphe, EC: external capsule, IPN: interpeduncular nucleus, LC: locus coeruleus, LDT: laterodorsal tegmental nucleus, LH: lateral hypothalamic area, MS: medial septal nucleus, PPT: pedunculopontine nucleus,

SN: substantia nigra. **(B)** Topographical connections between cholinegic neurons in brainstem nuclei and dopamainergic regions in midbrain. SNc receives cholinergic inputs from both PPT and LDT bilaterally. Ipsilateral and cotralateral cholinergic axons from the most rostral part of the PPT and LDT innervate SNc .Adapted from Mena-Segovia *et al.*, 2008.

ACh mediates pre- and postsynaptic responses through a wide variety of neuronal subtypes of ACh receptors in the brain. There are two types of ACh receptors (AChRs): G protein coupled muscarinic acetylcholine receptors (mAChRs) and nicotinic acetylcholine receptors (nAChRs), which are ligand-gated ion channels. (Dani and Bertrand, 2007; Wess, 2003). nAChRs are nonselective excitatory cation channels which open by binding to ACh or nicotine, which causes a conformational change in their structures resulting in the flux of $Na^+$, $K^+$, $Ca^{2+}$ down their electrochemical gradients (Figure 1.3B)(Dani and Bertrand, 2006). They belong to the superfamily of Cys-loop receptors that includes $GABA_A$, glycine, and 5-HT3 serotonin receptors (Nys et al., 2013). nAChRs are constituted from five transmembrane heteromeric or homomeric assemblies of α- and β-subunits that are arranged around a central pore (α2-α10 and β2-β4) (Figure 1.3C and D) (Dani and Bertrand, 2007). Each subunit consists of a large extracellular amino-terminal domain, followed by four transmembrane α-helical domains (M1-M4), and a short extracellular carboxy terminal. (Figure 1.3A). The major role attributed to nAChRs in the brain seems to be to facilitate the release of many different neurotransmitters (Mansvelder and McGehee, 2000; Mansvelder et al., 2002; Nelson et al., 2014; Parikh et al., 2010; Role and Berg, 1996; Wonnacott et al., 2006; Xiao et al., 2015a). Different subtypes of nAChRs such as α4β2, α6β2, α3β4, and α7 modulate the

release of GABA, glutamate, and DA (Exley and Cragg, 2008; Mansvelder and McGehee, 2000; Mansvelder et al., 2002, Nelson et al., 2014; Parikh et al., 2010).

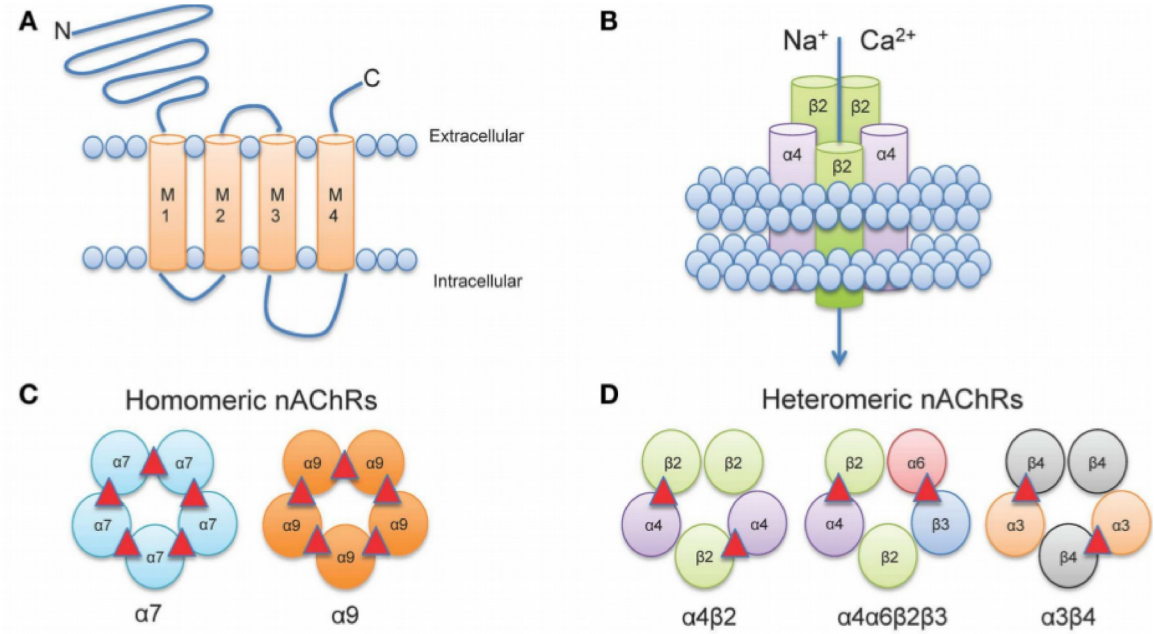


**Figure 1.3** Structure of the functional nAChR. (A) Membrane topology of a nAChR subunit. (B) A functional nAChR results from the assembly of five subunits around a central pore which nonselectively is permeable to cations. (C & D) Homomeric and heteromeric assemblies of α- and β-subunts. Red triangles show the ACh binding sites. Adapted from Hendrickson et al., 2013.

### 1.3.3 Cholinergic neurotransmission in the substantia nigra

The LDT and PPT are two brainstem cholinergic nuclei that play a major role in influencing the activity of DA neurons in the midbrain (Grace et al., 2007; Mena-Segovia et al., 2008). Neuroanatomical studies have shown that the projections from rostral PPT innervate the SNc, whereas the projections from caudal PPT and LDT innervate the VTA (Figure 1.2 B) (Dautan et al., 2014; Forster and Blaha, 2003; Oakman et al., 1995;

Oakman et al., 1999; Omelchenko and Sesack, 2005; Wang and Morales, 2009). Based on ultrastractural studies, it has been elucidated that there is synaptic connectivity between cholinergic afferents and DA and non-DA neurons in the SN (Garzón et al., 1999; Schäfer et al., 1998). As the earliest evidence of the role of the cholinergic system in modulating DA release, Scarnati and coworkers reported that electrical stimulation of PPT evoked excitation of both SNc and SNr neurons and was mediated by ACh and glutamate (Scarnati et al., 1984, 1986). Later on, Imperato et al. showed that nicotine could stimulate DA release onto the limbic system in a dose-dependent manner (Imperato et al., 1986). Multiple studies have revealed that the primary receptors for ACh in the SN are nAChRs, which include α6β2*, α4β2*, and α7 (*, channel may contain other subunits) (Champtiaux et al., 2003; Drenan et al., 2008; Nashmi et al., 2007a). Given the fact that the major role for nAChRs is to facilitate neurotransmitter release (Mansvelder and McGehee, 2000; Mansvelder et al., 2002), it has always been a challenging question how the cholinergic system modulates SN neuronal activity. In 2007, Nashmi and coworkers showed that chronic nicotine upregulates α4β2* localized in SNr GABAergic neurons (Nashmi et al., 2007). Moreover, nicotine can also modulate GABA release onto SNc DA neurons (Xiao et al., 2015a). Studies using mice with gain of function α6* receptors showed that activation of these receptors on SNc DA neurons caused an augmentation in DA neuronal excitability and hyperactivity in locomotor behaviour (Drenan et al., 2008). Over the last decade, many studies have reported that the loss of cholinergic neurons in the PPT results in a Parkinsonian phenotype due to significant loss of DA neurons in the SNc (Bensaid et al., 2016; Pienaar et al., 2013; Rinne et al., 2008).

It has also been documented that there is neuronal loss, especially of cholinergic neurons in the PPT of patients with PD (Hirsch et al., 1987; Pienaar et al., 2013, 2015). These data show that there are reciprocal interactions between cholinergic neurons and DA neurons which are vital for their survival. Although it has been well documented that exogenous activation of the cholinergic system strongly regulates DA neuron excitability and the transition to burst firing, we do not yet know how neuronal activity of the SN is modulated by endogenous release of ACh. Therefore, the contribution of the cholinergic system to SN function cannot be fully understood unless an approach eliciting endogenous ACh release is used. Here in this study a combination of optogenetics, that allows precise control of circuit function, electrophysiological and behavioural approaches were used to delineate the role of the cholinergic system in modulating SN neuronal activity.

### 1.3.4 Role of the basal ganglia in locomotion

The BG is a major brain region involved in the processing of locomotor behaviours. It is comprised of direct and indirect pathways which are two opposing pathways that originate from the striatum. D1 MSNs and D2 MSNs are the main initiators of direct and indirect pathways, respectively. These two pathways are thought to promote or suppress locomotor behaviour by either increasing or decreasing the activity of the motor cortex (Graybiel et al., 1994). Nevertheless, these classic models emphasize that the direct pathway facilitates while the indirect pathway inhibits voluntary movement. It is thought that the behaviour of cortical neuronal activity to shape a proper motor action is dependent on distinct factors, including “the fraction of cortical activity that is driven by

striatum-regulated thalamic inputs, the degree of tonic inhibition in the thalamus from ongoing SNr activity, and the speed with which cascading inhibitory networks disinhibit the thalamus and cortex" (Oldenburg and Sabatini, 2015). Olenburg and Sabatini examined the effects of optogentic stimulation of D1 MSNs or D2 MSNs on the primary motor cortex of mice during motor action. Consistent with the classic model, they found that the indirect and direct pathways of the striatum antagonized or enhanced motor cortical activity of neurons, respectively. However, at the level of individual neurons, cortical responses to activation of D1 and D2 MSNs were heterogeneous and context-dependent since trained movements and cues could blunt the effect of the direct pathway in modulating motor cortical activity (Oldenburg and Sabatini, 2015). In order to elucidate the distinct contributions of each pathway of the BG to modify movement, Freeze and coworkers (2013), using optogenetic approaches showed that activation of the direct pathway led to movement initiation correlated with inhibition of a subpopulation of SNr GABAergic neurons. Selective activation of the indirect pathway resulted in inhibition of movement and an increased firing rate of SNr neurons (Freeze et al., 2013). These results strongly suggest that SNr is one of the major output nuclei of the BG which can be stimulated or inhibited by striatal MSNs. As a matter of complexity in BG circuits, Cui et al., 2013 reported that both population of neurons (D1 and D2 MSNs) increased their firing rate when animals were in an active state and remained silent when animals were in a stationary state (Cui et al., 2013). These recent findings challenge the classical view of basal ganglia functions in controlling voluntary movement.

The SNc consists of bilateral nuclei in the ventral midbrain that are populated by

tightly clustered DA neurons. These DA neurons mainly project to the input structure of the BG, namely the dorsal striatum, and release DA, which regulates MSNs neuronal activity and has a key role in locomotor behaviour since the loss of DA in Parkinson's disease leads to profound voluntary movement deficits (Calabresi et al., 2014). In order to elucidate is the kinetics of DA signaling of incoming axons in the dorsal striatum during locomotion, Howe and Dombeck (2016) used GCaMP6f, a genetically encoded calcium indicator, and channelrhodopsin (ChR2) approaches to image DA projecting axons in the dorsal striatum by two-photon microscopy. They found that treadmill locomotion was associated with widespread and synchronous sub-second increases in DA release from DA axons that originated from the SNc (Howe and Dombeck, 2016). They also showed that signaling through DA axons in the dorsal striatum resulted in locomotion initiation in less than 200 ms (Howe and Dombeck, 2016). These results have revealed the importance of SNc DA neurons in modifying locomotor behaviour at a sub-second time scale. Furthermore, it has been shown that the activity of DA neurons can change during locomotion in a heterogeneous manner, suggesting there may be a selective encoding of different types of movements by activation of different subpopulation of DA neurons (Barter et al., 2015; Dodson et al., 2016a; Jin and Costa, 2010). For instance, some DA neurons in the SNc have a pause in activity during the onset of movements, suggesting a strong and rapid change in DA concentration in the dorsal striatum, which may be vital for movement initiation (Dodson et al., 2016).

### 1.3. 5 Role of the cholinergic system and nAChRs in locomotion

One of the functional circuits in which the cholinergic system of the brainstem may

modulate locomotor activity is the PPT and medioventral medulla (MED) neuronal circuit. Depolarization of glutamatergic neurons in the MED is contributed by cholinergic input from the PPT (Mamiya et al., 2005; Skinner et al., 1990). It was reported that activation of muscarinic ACh receptors on brainstem cholinergic neurons has a modulatory effect on locomotor activity (Brudzynski et al., 1988; Smetana et al., 2010). Previous studies have shown that there are two populations of neurons in the PPT whose activity responds differentially to movement (Matsumura et al., 1997; Norton et al., 2011). There were PPT neurons whose action potential firing was positively correlated to movement, while there were also other PPT neurons with neuronal activity negatively correlated to movement (Matsumura et al., 1997; Norton et al., 2011). It is unclear how a cholinergic nucleus such as the PPT can mediate a seemingly paradoxical effect of both stimulation or inhibition of locomotor activity. Interestingly, although optogenetic activation of cholinergic neurons in the brainstem can positively modulate locomotion, they are less effective in driving the initiation of movement within a short latency less than a second (Roseberry et al., 2016). However, a different study has indicated that optogenetic activation of PPT cholinergic terminals ending in the SNc and VTA can stimulate motor activity and reward reinforcement (Xiao et al. 2016). However, photostimulation of LDT cholinergic terminals is less effective in modifying locomotion but more critical in producing reward behaviours mediated by the VTA (Xiao et al. 2016). Recently, it was shown that activation of PPT and LDT cholinergic terminals in the midbrain produce opposing effects on locomotor activity; PPT transiently increased while LDT decreased locomotion in freely moving rats in an open field, however, the exact

mechanism was unclear (Dautan et al., 2016b).

nAChRs are widely expressed in the SN and their activation *in vitro* causes depolarization and increased firing in DA neurons (Nashmi et al., 2007a). Moreover, lesioning the LDT decreased locomotor activity in rats and abolished nicotine's effect on modulating locomotion (Alderson et al., 2005). This indicates that the LDT and nAChRs play a key role in modulating locomotor behaviour. Studies using mice with gain of function α6* nAChRs showed that activation of these receptors on DA neurons in SNc causes an augmentation in DA neurons excitability and hyperactivity in locomotor behaviours (Drenan et al., 2010). Other studies reported that β2 knock-out mice showed hyperactivity in open field locomotion which can be reversed by genetic rescue of the β2 nAChR subunit in SNc (Avale et al., 2008; Granon et al., 2003). These results show that nAChRs in the SNc are necessary for normal locomotion behaviour, however little is known about how neuronal activity of the SNc is modulated by endogenous release of ACh.

### 1.3.6 Hypotheses

The primary hypothesis that I will test is that endogenous release of ACh modulates SNc activity differentially depending on presynaptic or postsynaptic activation of nAChRs in SNc. Secondly, I hypothesize that DA neurons in distinct regions of the SNc, medial SNc and lateral SNc, will be modulated differentially by cholinergic inputs. Finally, I hypothesize that medial and lateral SNc DA neurons will have distinct effects in mediating locomotion due to differential cholinergic mediated neurotransmission in these regions.

# Chapter 2- Materials and Methods

## 2.1 Mice

Experiments were performed using ChATcre-ChR2 mice which are produced from the cross of ChAT-cre mice (JAX stock# 006410), knock-in mice which express cre-recombinase driven by the endogenous choline acetyltransferase (ChAT) promotor, with a knock-in cre-dependent channelrhodopsin-yellow fluorescent protein chimera (ChR2) mouse line (JAX stock# 012569). This mouse line is a knock-in so homozygous has normal expression of ChAT. The other mouse line used in this study was ChAT cre-ChR2-VGAT KO, which was produced from the cross of $Vgat^{flox}$ (JAX stock# 012897) and ChAT cre-ChR2 mice. We also used ChAT-tdTomato mice, a cross between ChAT-cre and Ai9 mice (JAX stock# 007909). α4YFP knock-in mice (Nashmi et al., 2007) and C57BL/6J mice were also used. All the mice were housed under a 12 h light/dark cycle and were given *ad libitum* access to both food and water. All experimental procedures were conducted in accordance with the Canadian Council for Animal Care and a protocol which was approved by the Animal Care Committee of the University of Victoria.

## 2.2 Brain slice preparation for electrophysiology

Acute brain slices were acquired from mice aged 20-25 days old. Mice were anesthetized by isofluorane inhalation and rapidly decapitated. Brains were removed and held for 30 sec in cold (2–4°C) cutting solution containing: 92 mM N-methyl-D-glucamine (NMDG), 2.5 mM KCl, 1.25 mM $NaH_2PO_4$, 30 mM $NaHCO_3$, 20 mM HEPES, 4.5 mM D-glucose, 5 mM Na-ascorbate, 3 mM Na-pyruvate, 0.5 mM $CaCl_2$, and 10 mM $MgCl_2$

(pH between 7.3-7.4). The brain was blocked in melted 3% agar-A (CAS#9002-18-0, Bio Basic Canada Inc), then placed on the slicing platform and sectioned coronally at 320 µm thickness with a vibratome (Leica VT 1000S) containing cold (2–4°C) bubbled (95% O2/5% CO2) cutting solution. Sections that included the SNc were transfered into continuously carbogenated pre-warmed (32–34°C) cutting solution for a period of 12 min time for initial recovery. Then the slices were transferred into a room temperature carbogenated holding solution containing: 119 mM NaCl, 2.5 mM KCl, 1.2 mM $NaH_2PO_4$, 24 mM $NaHCO_3$, 12.5 mM D-glucose, 5 mM Na-ascorbate, 3 mM Na-pyruvate, 2 mM $CaCl_2$, and 2 mM $MgCl_2$ for period of 30 min as second recovery before recording.

## 2.3 Electrophysiological recordings

A brain slice was transferred onto a recording chamber on an upright Nikon FN1 microscope equipped with a CFI APO 40X W NIR objective (0.80 numerical aperture, 3.5 mm working distance). The chamber was continuously perfused with 32°C carbogenated recording solution containing: 122 mM NaCl, 2.5 mM KCl, 1.2 mM $NaH_2PO_4$, 24 mM $NaHCO_3$, 12.5 mM D-glucose, 5 mM Na-ascorbate, 3 mM Na-pyruvate, 2 mM $CaCl_2$, 0.1 mM $MgCl_2$. In select experiments muscarinic acetylcholine receptors were inhibited with 100 nM atropine to confirm nAChR currents (SKU# A0132, Sigma-Aldrich). DA neurons were visualized in the SNc via video monitored infra-red differential interference contrast illumination microscopy using the 40X objective. Whole-cell patch-clamp recordings were performed using patch pipettes with resistances between 5-8 MΩ. Recording pipettes were prepared from borosilicate glass

capillaries (1B150F-4, WPI, USA) and for current-clamp recordings they were filled with pipette solution (280–290 mOsm/L, pH 7.4) containing: 130 mM K gluconate, 5 mM EGTA, 10 mM HEPES, 2 mM $MgCl_2$, 0.5 mM $CaCl_2$ $2H_2O$, 5 mM phosphate Tris, 3 mM Mg-ATP, and 0.2 mM GTP Tris. For voltage-clamp recordings the pipettes were filled with a modified pipette solution (280–290 mOsm/L, pH 7.4) containing: 135 mM $CsMeSO_4$, 5 mM QX314 chloride, 0.6 mM EGTA, 10 mM HEPES, 2.5 mM $MgCl_2$, 5 mM phosphate Tris, 3 mM Mg-ATP, and 0.2 mM GTP Tris. All the recordings were amplified using a MultiClamp 700B amplifier (Molecular Devices), low-pass filtered at 4 kHz, sampled at 10 kHz with a Digidata 1440A data acquisition system (Molecular Devices) and recorded using pCLAMP 10.2 acquisition software (Molecular Devices). For recording evoked excitatory postsynaptic currents (eEPSCs) and evoked inhibitory postsynaptic currents (eIPSCs) cells were held at -70 mV and -20 mV, respectively, after correction for liquid junction potential and the series resistance was corrected 40%. In the current-clamp mode bridge balance and capacitance neutralization were applied. In some recordings, biocytin (0.5%) (Cat. # 3349, Tocris Bioscience) was in the recording pipette.

## 2.4 Optogenetic stimulation of brain slices

After establishing whole-cell recording and identifying DA neurons, in order to stimulate ChR2-containing cholinergic axons, we used 5 ms wide-field illumination through the 40X objective with a 470 nm blue LED (Thorlabs, part # M470L3-C5). Square pulses of blue light, at half-maximum intensity, were controlled by a controller box which was driven by pCLAMP 10.2 (Molecular Devices) through Digidata 1440 (Molecular Devices). To evaluate the effects of endogenous release of ACh on DA neurons, we

stimulated cholinergic axons with the 5 ms pulse at a 5 Hz or 15 Hz stimulation train for a train duration of 1.5 sec and repeated every 30 sec.

## 2.5 Optical fiber implant construction for *in vivo* optogenetics

To construct implantable optical fibers, we used step-index multimode fiber (200 µm core, 0.5 NA, Thorlabs, Item# FP200URT). Using a microstripper (Thorlabs, Part# T12S21), we stripped ~30 mm of fiber and then cut it with a fiber cutter, while leaving 10 mm of unstripped fiber. One drop of heat-curable epoxy (Thorlabs, Part# F112) was placed at the flat side of a ceramic ferrule (Precision Fiber Products, Inc, SKU: MM-FER2007C-2300) and the stripped end of the fiber was inserted through the ferrule. Twelve mm of the stripped fiber was left exposed and the epoxy was cured with a heat gun. The ferrule with fully cured epoxy was secured from the unstripped end to a flat surface by a piece of scotch tape and then the fiber at the convex end of the ferrule was scored with a fiber cutter as well as the stripped end (8 mm or 5 mm in length). To polish the convex end of the implantable optic fiber, we used a hemostat to hold the ferrule perpendicular to polishing paper and made 20 eight-shaped rotations. We used four grades of polishing paper in the order of 5, 3, 1, and 0.3 µm (Thorlabs, Part# LF5P, LF3P, LF1P, and LF0.3P). The optic fibers with concentric light transmission and > 60% light output of the input light from the patch cable were considered acceptable for implantation.

## 2.6 Surgery for optical fiber implantation

The ChATcre-ChR2 and α4YFP mice, aged between 70 to 120 days old, were anesthetized with inhaled 2% isofluorane using an anesthetic machine. To make sure the

animal was deeply anesthetized we tested for the lack of a toe pinch reflex. The anesthetized mouse was placed and stabilized on a stereotaxic frame (SKU# 51615, Stoelting Co.) and sufficient amount of tear gel was applied to mouse eyes to minimize drying. Fifty µl of lidocaine was injected underneath the scalp and then a 1 cm midline incision was made through the scalp. The mouse head was leveled by measuring bregma and lambda dorsal-ventral coordinates. A bone anchor screw (SKU# 51462, Stoelting Co.) was inserted into the skull 3.5 mm caudal from the optic fiber insertion site to ensure a properly secured headcap. Two holes were drilled bilaterally into the skull for either the medial SNc (bregma 3.25 mm, lateral ±0.70 mm, ventral 4.15 mm) or lateral SNc (bregma 3.25 mm, lateral ±1.35 mm, ventral 3.9 mm). The implantable optic fiber was attached to a stereotaxic cannula holder (SCH_1.25, Doric Lenses) and lowered into the brain (ventral: 4.15 mm for medial SNc and 3.90 mm for lateral SNc). For the medial SNc, in order to fit these two closely spaced optic fibers, first we implanted the shorter (5 mm long) optic fiber and then the longer (8 mm) one. Optic fibers, were then glued with cyanoacrylic glue and then a sufficient amount of dental cement was applied with a spatula. After ~10 min the incision was sutured and the mouse was put under red light in a clean cage and monitored for full recovery. Approximately 7 days after surgery, we commenced the optogenetic behavioural experiments.

## 2.7 Open-field locomotor behaviour test

Experiments were performed in a dark room lit by a red lamp. Video recordings were performed with a video camera (Sony Digital HD video camera recorder, Handycam, HDR-SR1) mounted 70 cm above a 42 cm x 20 cm cage. Individual mice were placed in

the cage at least 10 min before testing to acclimatize to the new environment. To deliver blue light for stimulating ChR2-containig axons in the SNc, a 470 nm blue LED (cat# M470F3, Thorlabs) was attached to a monofiber optic patch cord (cat# MFP-200/220/900-0.53-1m-FCM-SMA, Doric Lenses), then to a fiber optic rotary joint (cat# FRJ-1x1-FC-FC, Doric Lenses) and then to a branched fiber optic pach cord (BFP(2)-200/220/900-0.53-1m-FCM-2xZF1.25(F), Doric Lenses), which was connected to the implanted optic fibers with zirconia ceramic sleeves (cat# SM-CS125S, Precision Fiber Products Inc). LED blue light was delivered at 5 ms square pulse durations set at maximal intensity using a custom made LED driver box, which was triggered with a Grass S48 stimulator (Grass Instruments). Each open field test took 25 min and comprised of 5 min baseline locomotor activity, 5 min locomotor activity during discontinious photostimulation at 5 Hz, 5 min recovery, 5 min locomotor activity during discontinious photostimulation at 15 Hz, and 5 min recovery (Fig. 2.1). The discontinuous photostimulation consisted of two 1 min of photostimulation and a 40 sec photostimulation period, which were preceded by 20 sec and interspaced by 1 min of no photostimulation (Fig. 2.1). The recorded videos were analysed using ImageJ software (version 1.50i, https://imagej.nih.gov/ij/). The videos were converted to avi files using FFmpeg software. The stack of images for each video was converted to 8 bit grey scale Gaussian blur filtered at 5 and thresholded to detect the mouse body. The center of mass X and Y coordinates of the thresholded mouse body in each frame was calculated using the “Analyze particles” function. From this the total distance travelled for each mouse was calculated.

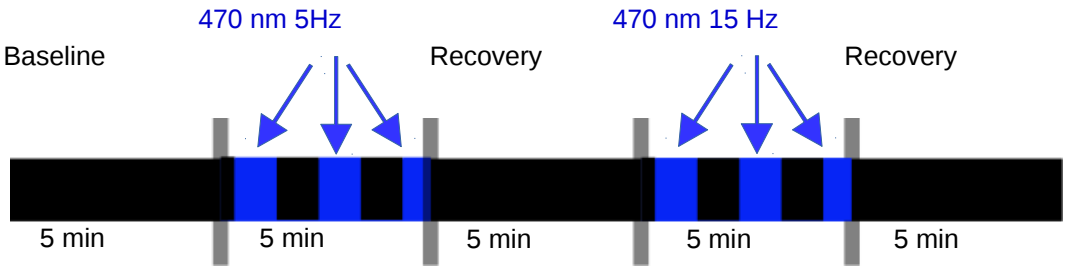


**Figure 2.1** Experimental design for open field test in mice implanted with optical fiber.

## 2.8 Immunohistochemistry

Mice were anaesthetized with ketamine (100 mg/ml) and dexmedetomidine hydrochloride (0.5 mg/ml) and intracardially perfused with 20 ml PBS with heparin (pH= 7.6), followed by 25 ml of 4% paraformaldehyde (PFA) in phosphate buffered saline (PBS) (pH= 7.6) and 20 ml of 5% sucrose in PBS (pH= 7.6). The brain was extracted and kept in 30% sucrose (pH= 7.6) for 24 hrs, frozen in O.C.T. mounting compound and then sectioned coronally 30-40 µm thick with a cryostat and mounted on coated slides (cat# 15-188-48, Superfrost Plus Gold, Fisher Scientific). For the fiber optic implanted mice, they were intracardially perfused with 20 ml PBS with heparin (pH= 7.6), followed by 25 ml of 4% PFA. The extracted brains were then post-fixed overnight in 4% PFA in PBS, then cut 50-60 µm thick coronal slices in PBS with a vibratome (VT1000 S, Leica). The slices, contaning optic fiber tracts, were used for immunohistochemistry.

The slides with brain cryostat sections were thawed for 7 min, washed twice with PBS (10 min each), and then incubated with 0.25% Triton-X for 7 min. The slides were washed twice for 10 min with PBS and then blocked with 10% donkey serum in PBS for

30 min. All primary antibodies were diluted in 3% donkey serum in PBS at 1:250 dilution. For detecting DA neurons in the SNc, the slides were incubated with a primary antibody against tyrosine hydroxylase (Pel-Freez, cat# P4010-0, host: rabbit; abcam, cat# AB76442, host: chicken; Millipore, cat# AB1542(CH), host: sheep), GABA antibody (abcam, cat# AB62669, host: chicken), GAD67 monoclonal antibody (Millipore, cat# MAB5406, host: mouse) and ChAT for 24 hrs at 4ºC. To evaluate the extent of ACh and GABA colocalization in the cholinergic terminals in the SNc of C57BL/6J mice, we used primary antibodies against vesicular acetylcholine transporter (VAChT) (Millipore, cat# ABN100, host: goat) and vesicular GABA transporter (VGAT) (Millipore, cat# AB5062P, host: rabbit). After incubation with primary antibodies, slides were washed with PBS three times (10 min each) and incubated with a secondary antibody (Alexa Fluor 405 IgG secondary antibody, Invitrogen, cat# A-31556; Alexa Fluor 488 IgG secondary antibody, Cy5 IgG secondary antibody, Jackson ImmunoResearch Labs, cat# 715-175-150) diluted in 3% donkey serum (diluted in 1x PBS) at a 1:300 concentration and incubated for 24 hrs at 4 ºC. Brain slices were then washed with PBS three times (15 min each) and then dried out for 2 min in 37 ºC before mounting coverslips with 30 µl Immu-Mount, pH= 8.2, (cat# 9990402, Thermo Scientific Shandon).

To visualize recorded DA neurons filled with biocytin, brain slices were fixed in 4% paraformaldehyde (pH= 7.6) in PBS for 24 hrs at 4°C. The slices were washed three times with PBS (10 min each), and then incubated with 0.25% Triton-X for 10 min. After twice washing with PBS (5 min each), the slices were transfered into 10% donkey serum for 30 min and then they were incubated with Alexa Fluor 555 conjugated streptavidin at

a 1:300 concentration, (cat# S32355, Thermo Fisher Scientific) for 24 hrs at 4°C. The slices were then washed three times with PBS, placed on slides, dried and mounted with 30 µl Immu-Mount.

## 2.9 Confocal microscopy and colocalization analysis

Coverslipped slides were imaged using a Nikon C1si spectral confocal microscope. A 20X CFI Plan Apochromat (0.75 NA, 1.0 mm working distance) and 60X oil CFI Plan Apo VC objectives (1.40 NA, 0.13mm working distance) were used to acquired images. Lambda-stack images were collected simultaneously with one laser sweep onto an array of 32 photomultiplier tubes, each sampling a 5 nm wavelength band that spanned in total over 150 nm band width. Images were obtained at 512 pixels x 512 pixels with the pixel dwell time of 5.52 µsec and a spectral detector gain at 220. The pinhole was set to medium (60 µm diameter) and 405, 488 and 560 nm laser lines were used at intensities that did not saturate the signal. Analysis of colocalization of cholinergic and GABAergic terminals using confocal microscopy images was performed with ImageJ software, version 1.51a. Images were converted to 8-bit and a Gaussian blur filter set to 1.0, was applied to all images of the stacks. Automated thresholding was applied that successfully selected all puncta while maximally excluding background noise for the majority of slices. Corresponding thresholded slices from both labeled stacks were analyzed using JACoP colocalization plugin, which calculated two Manders coefficients (M1: proportion of pixels from image A overlapping with pixels from image B; M2: proportion of pixels from image B overlapping with pixels from image A). As a control experiment, the slices were re-analyzed using JACoP after rotating one of the images 90 degrees relative to the

other image. This was done to rule out the possibility that the overlap found in the correct orientation was due to chance rather than true colocalization. Truly colocalized pixels should be moved out of alignment after rotation resulting in a decrease in Manders coefficients, while the amount of random overlap should remain very similar and therefore have similar Manders coefficients before and after rotation.

## 2.10 Statistical Analyses

Values are expressed as mean ± standard error. Statistics were analyzed with R statistical analysis software (www.r-project.org). Parametric statistical comparison tests were performed provided the data were normally distributed as determined by the Shapiro-Wilk test and the variances of the groups of data did not significantly differ from each other as determined with the Fligner-Killeen test of homogeneity of variances. Otherwise, non-parametric statistical tests were performed. To compare between two groups of data, a one tailed t-test or paired t-test was used assuming parametric criteria, while a Wilcoxon rank-sum test or repeated Wilcoxon rank sum test were used for non-parametric data. To analyze the means of more than two groups that were repeated over different conditions, a one-way repeated measures ANOVA was used for parametric data, while a Friedman rank sum test was used for non-parametric data. Post-hoc analyses were either a Tukey HSD or t-tests with Bonferroni correction for parametric data, while Wilcoxon rank sum tests were performed on nonparametric data. Data were considered significantly different at $p < 0.05$.

# Chapter 3- Cholinergic neurotransmission in different subregions of the substantia nigra differentially controls DA neuronal excitability and locomotion

## 3.1 Results

### 3.1.1 DA neurons in the medial and lateral SNc display different biophysical properties

To examine the heterogeneity of DA neurons in spatially distinct regions of the SNc, we peformed whole-cell patch-clamp recordings of DA neurons from two different regions of SNc -- medial and lateral SNc. The medial lemniscus (ml) was used as the landmark separating VTA from SNc and the oculomotor nerve was the landmark that separated medial from lateral SNc (Fig. 3.1E). DA neurons were characterized by slow tonic firing frequency (< 5 Hz), a broad action potential (> 2 ms) and a hyperpolarization-activated inward current (Ih) (Fig. 3.1A-D). With biocytin in the recording pipette (Fig. 3.1F-K), it was evident from the recordings that medial and lateral DA neurons were distinct based on morphological and electrophysiological properties. In the lateral SNc, DA neuronal somata were fusiform with resting membrane potentials of -54.1 ± 1.4 mV, large Ih currents (-1071 ± 190 pA), and average firing frequency of 3.2 ± 0.7 Hz are mostly dominant (Table 3.1). Medial DA neurons were, multipolar with more hyperpolarized resting membrane potentials (-57.2 ± 0.5 mV) ($p = 0.01$, $t(16) = 2.54$), smaller Ih currents (-662 ± 137 pA) ($p = 0.04$, $t(20) = 1.79$), and lower firing frequency of 1.4 ± 0.3 Hz ($p = 0.03$, Wilcoxon rank sum test) (Table 3.1).

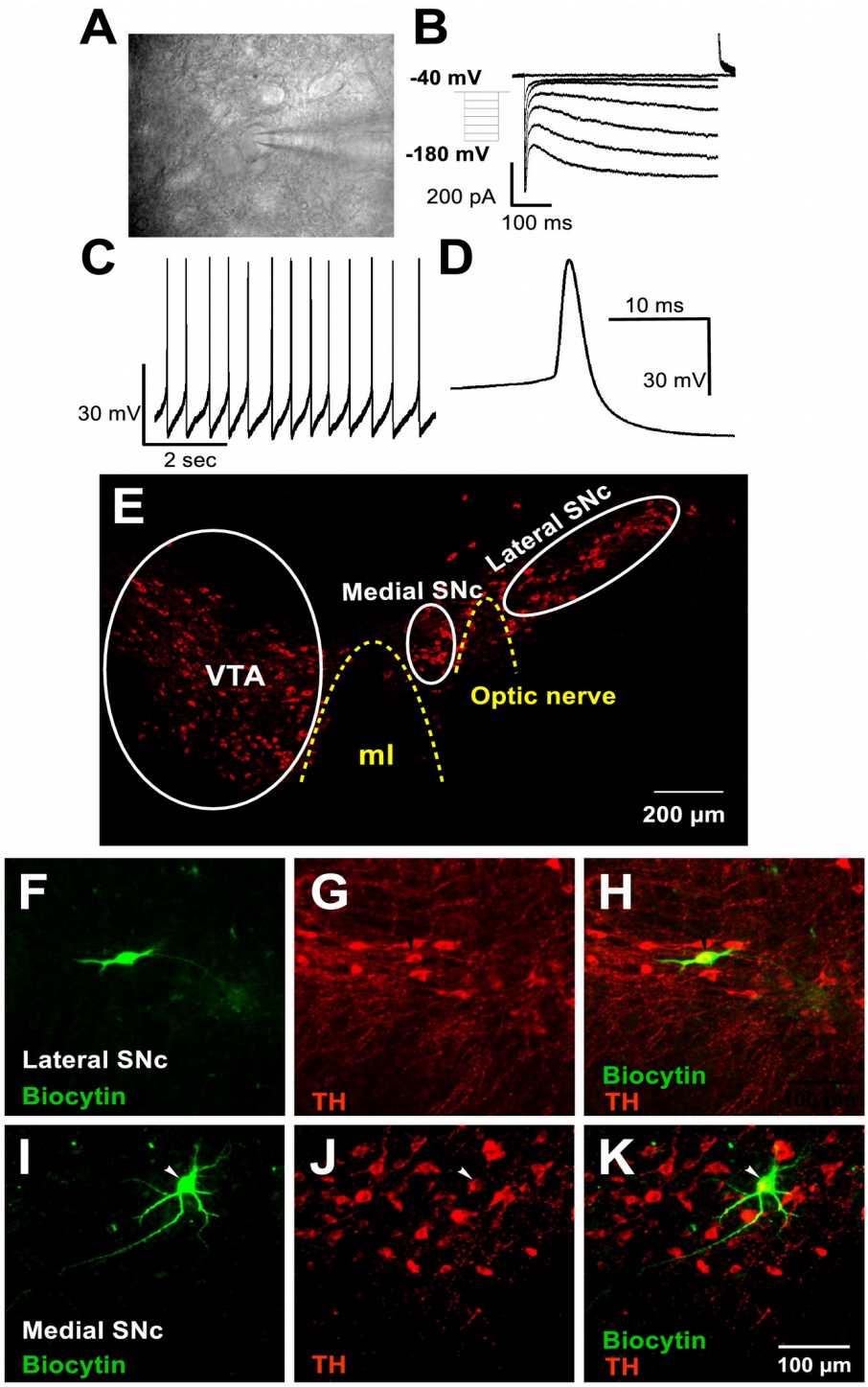


**Figure 3.1.** Identification DA neurons in SNc (A) IR DIC image of a recorded DA neuron in lateral SNc. (B-D) DA neuronal recording in the lateral SNc showing an Ih current, low firing frequency (~1.5 Hz) and a broad action potential (~3 ms half width). (E) Anatomical distribution of medial and lateral SNc neurons were identified with TH

staining. (F-H) A DA neuron in the lateral SNc with a fusiform soma revealed by biocytin labeling via patch clamp whole cell recordings. (I-K) A DA neuron in the medial SNc with a multipolar soma. Scale bar = 100 µm.

### 3.1.2 Stimulation of cholinergic terminals in the lateral SNc mediates mainly excitatory currents on DA neurons

We recorded from SNc DA neurons in mouse brain sections from ChATcre-ChR2 mice to examine how cholinergic neurotransmission modifies dopaminergic activity. In this mouse line, ChR2 is expressed only in cholinergic neurons as verified with immunohistochemistry for ChAT (Fig. 3.2). We also verified by recording blue light evoked inward ChR2 mediated currents and their changes in excitability in LDT and PPT cholinergic neurons (Fig. 3.3, 3.4).

**Table 3.1.** Biophysical properties of DA neurons in the medial and lateral SNc.

| | **Lateral (n=8 cells, 7 mice)** | **Medial (n=10 cells, 7 mice)** | **p value** |
|---|---|---|---|
| V rest (mV) | -54.1 ± 1.4 | -57.2 ± 0.5 | 0.01 |
| R input (MΩ) | 290 ± 54 | 125 ± 21 | 0.003 |
| Ih (pA) | -1071 ± 190 | -662 ± 137 | 0.04 |
| AP amplitude (mV) | 77.8 ± 3.6 | 81.1 ± 3.4 | 0.26 |
| AP half width (ms) | 2.1 ± 0.2 | 3.0 ± 0.2 | 0.008 |
| AP freq (Hz) | 3.2 ± 0.7 | 1.4 ± 0.3 | 0.03 |

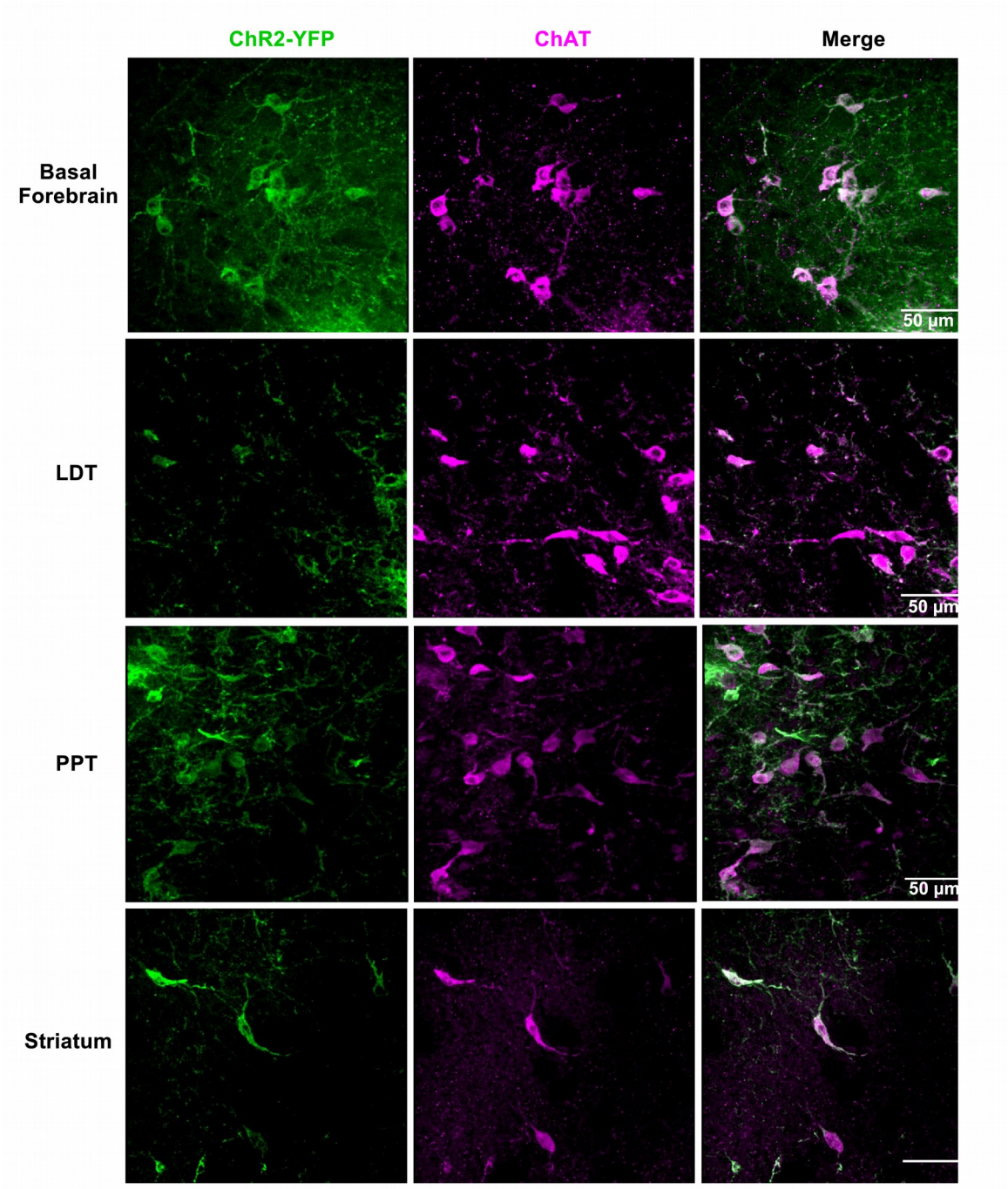


**Figure 3.2.** Validation of expression of ChR2 in only cholinergic neurons using ChAT-ChR2 knock-in mice. Immunohistochemistry for ChAT in ChAT-ChR2 mice showed that ChR2 is exclusively expressed in cholinergic neurons in different brain regions throughout the brain. Scale bar = 50 µm.

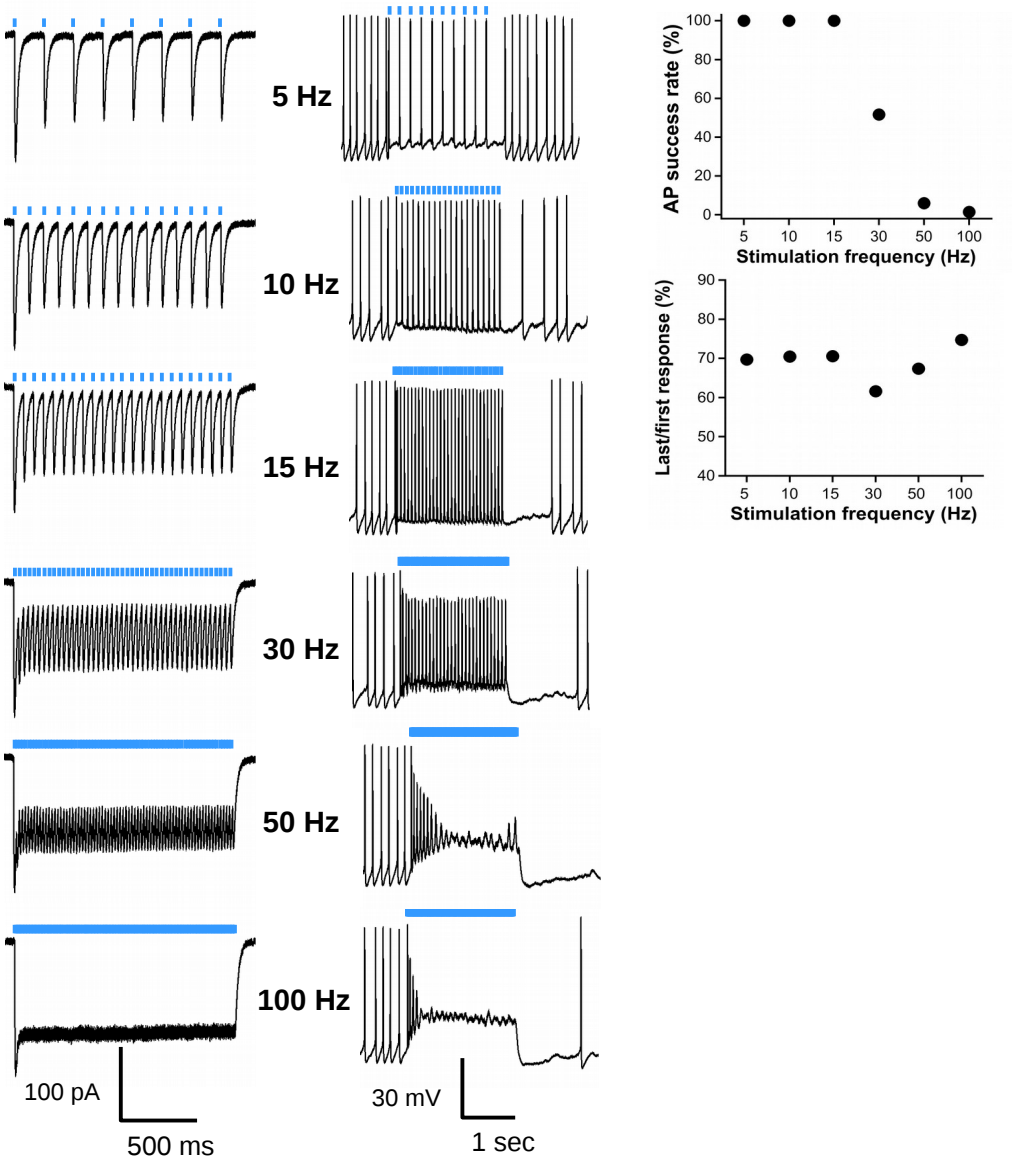


**Figure 3.3.** Frequency-dependent optogenetic modulation and recording of PPT cholinergic neurons. Left traces: voltage-clamp recordings showing different stimulation frequency trains of 5 ms pulsed blue light is sufficient to evoke inward ChR2 currents at different frequencies. Middle column traces: current-clamp recordings showing that ChR2-YFP expressing cholinergic neurons in the PPT are able to follow blue light stimulation reliably at 5, 10, and 15 Hz, but not at higher stimulation frequencies. Right top graph shows action potential success rate (%) in response to blue light stimulation at different frequencies. Right bottom graph shows the percentage change in the last blue light evoked ChR2 current as a percentage of the first one.

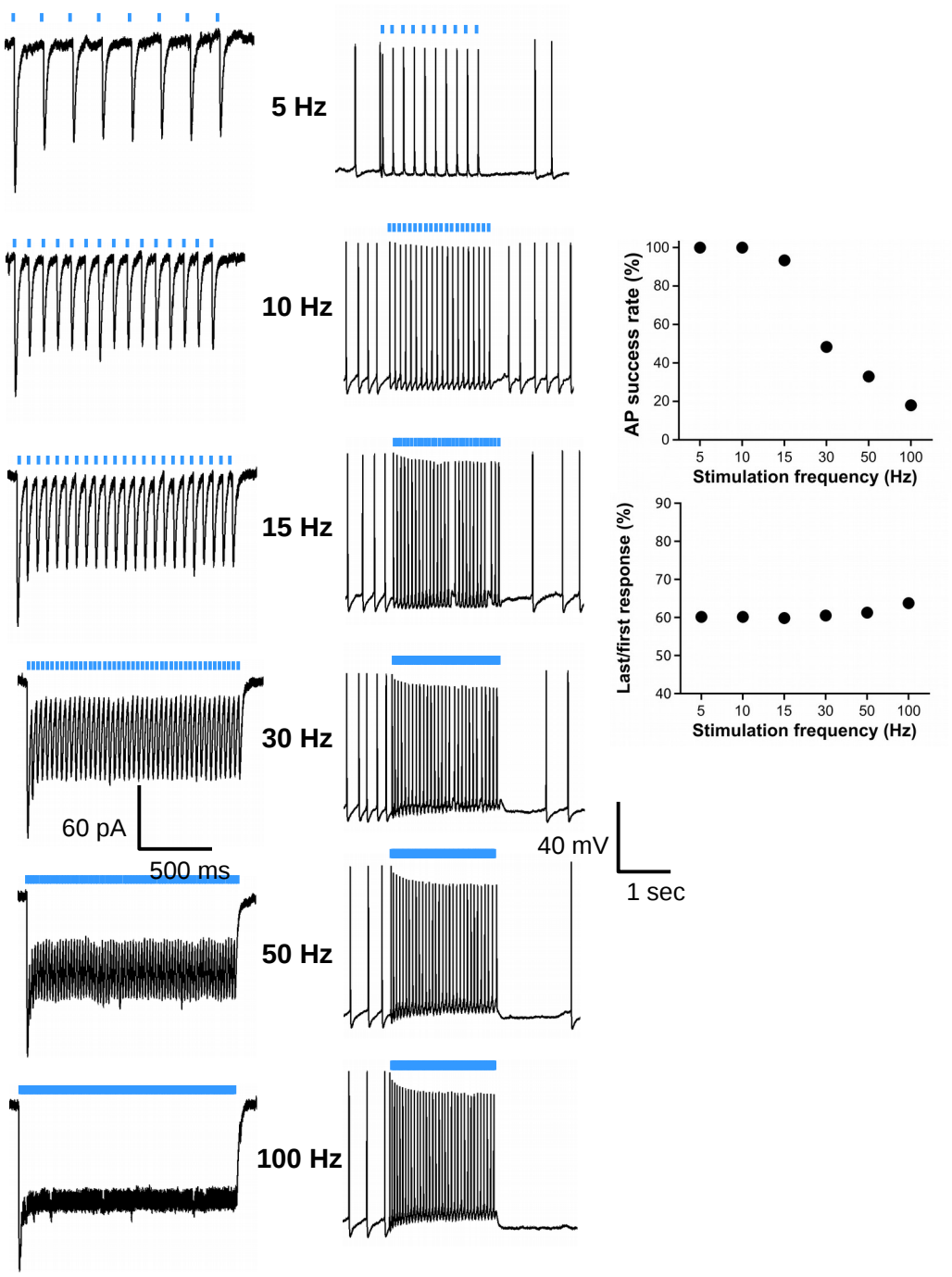


**Figure 3.4.** Frequency-dependent optogenetic modulation and recording of LDT cholinergic neurons. Left traces: voltage-clamp recordings showing different stimulation frequency trains of 5 ms pulsed blue light is sufficient to evoke inward ChR2 currents at different frequencies. Middle column traces: current-clamp recordings showing that ChR2-YFP expressing cholinergic neurons in the LDT are able to follow blue light stimulation reliably at 5, 10, and 15 Hz, but not at higher stimulation frequencies. Right

top graph shows action potential success rate (%) in response to blue light stimulation at different frequencies. Right bottom graph shows the percentage change in the last blue light evoked ChR2 current as a percentage of the first one.

Whole cell voltage-clamp recordings from DA neurons in acute brain slices showed that stimulation of cholinergic terminals in the lateral SNc by brief pulses of blue light elicited robust excitatory postsynaptic currents (EPSCs) held at −70 mV. About 92% of recorded neurons in the lateral SNc received excitatory nAChR mediated cholinergic neurotransmission (Table 3.2). These EPSCs included both monosynaptic (direct) nAChR or disynaptic (indirect) glutamatergic currents, which were both blocked by a cocktail of nAChR antagonists (DHβE, MLA, and MEC) (Fig. 3.5A1, A2), while only the latter were blocked by a glutamatergic antagonist cocktail of CNQX and AP5 (Fig. 3.5B1, B2). Furthermore, applying MLA (a specific α7 nAChR antagonist) revealed that the disynaptic glutamatergic currents were dependent on α7 nAChRs (data not shown).

Moreover, we confirmed the monosynaptic nicotinic and disynaptic glutamatergic currents by recording blue light evoked currents at different holding potentials from -100 mV to +40 mV in order to analyze the I-V relations for these currents. For the glutamatergic currents, the I-V curves had two components separated in time. The earlier component had a linear I-V relationship that reversed near 0 mV, which was characteristic for AMPA currents (Fig. 3.5C). The delayed component had a non-linear I-V relationship, which also reversed around 0 mV but rectified at hyperpolarized potentials, characteristic of an NMDA current (Fig. 3.5C).

In addition to cholinergic mediated EPSCs, 30% of the cholinergic stimulated responses also resulted in nAChR mediated disynaptic inhibitory postsynaptic currents

(IPSCs) when DA neurons were held at -20 mV (Table 3.2). These GABAergic currents were completely abolished by either the $GABA_A$ inhibitor gabazine or the cocktail of nAChR inhibitors.

**Table 3.2.** Breakdown of pharmacological sensitivities of cholinergic mediated currents following optogenetic activation of cholinergic terminals in the lateral SNc.

| | **Response in lateral region of SNc** | **Blocked by glutamate receptor inhibitors** | **Blocked by nAChR inhibitors** | **Blocked by $GABA_A$ Inhibitors** |
|---|---|---|---|---|
| **Inward** | 51 | 15 | 51 | 0 |
| **Outward** | 6 | 0 | 6 | 6 |
| **Biphasic** | 16 | 5(inward blocked) | 16 (inward and outward blocked) | 16 (outward blocked) |
| **Total # of cells** | 73 | 20 | 73 | 22 |

**Table 3.3.** Breakdown of pharmacological sensitivities of cholinergic mediated currents following optogenetic activation of cholinergic terminals in the medial SNc.

| | **Response in medial region of SNc** | **Blocked by glutamate receptor inhibitors** | **Blocked by nAChR inhibitors** | **Blocked by GABAA Inhibitors** |
|---|---|---|---|---|
| **Outward** | 42 | 0 | 42 | 42 |
| **Biphasic** | 34 | 0 | 31 (only inward not outward blocked)<br>3 (inward and outward blocked) | 34 (outward blocked) |
| **Inward** | 5 | 1 | 5 | 0 |
| **Total # of cells** | 81 | 1 | 81 | 76 |

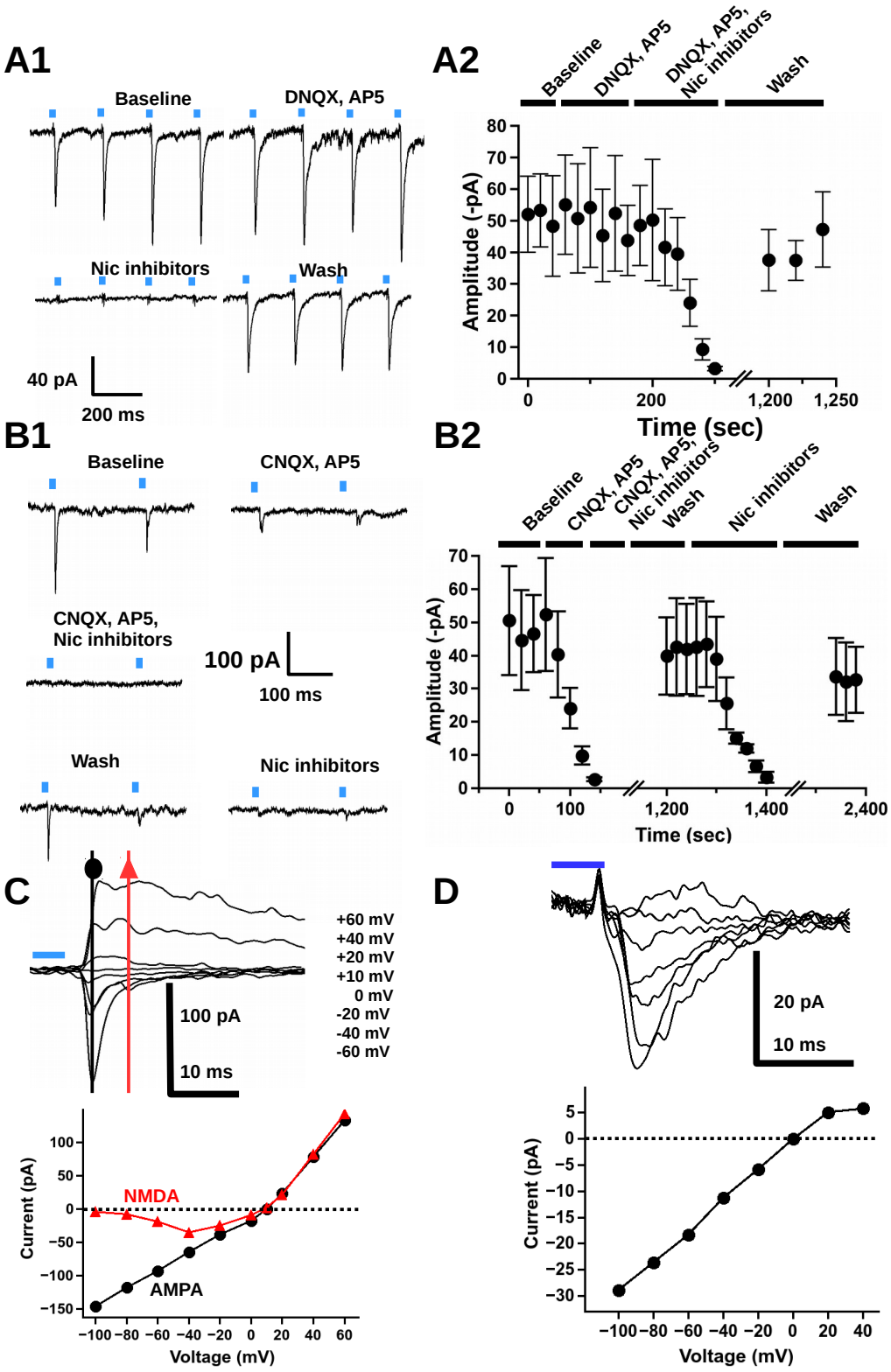


**Figure 3.5.** Lateral SNc expresses mainly excitatory glutamatergic and nicotinic mediated cholinergic neurotransmission.

(A1) Voltage-clamped traces showing that LED blue light activation (5 ms pulse duration, blue bars) of cholinergic terminals in the lateral SNc elicits nAChR currents that are insensitive to DNQX and AP5 but completely inhibited by the nAChR inhibitor cocktail of MEC, MLA and DHβE. Holding potential is -70 mV. (A2) A time course plot summarizing the data. (B1) Current traces from a neuron showing a disynaptic glutamatergic EPSC mediated by presynaptic nAChRs as evidenced by inhibition with CNQX and AP5 and the cocktail of nAChR antagonists. (B2) A summary plot showing the time course of inhibition of the glutamatergic responses with CNQX and AP5 and nAChR antagonists. (C) An example of blue light evoked disynaptic glutamatergic responses at different holding potentials. The corresponding I-V plot at the earlier (black circles) and latter (red triangles) time points display AMPA and NMDA currents, respectively. (D) Current traces of nAChR responses at different holding potentials (-100 to +40 mV) and the corresponding I-V relationship, which shows rectification of current at positive holding potentials.

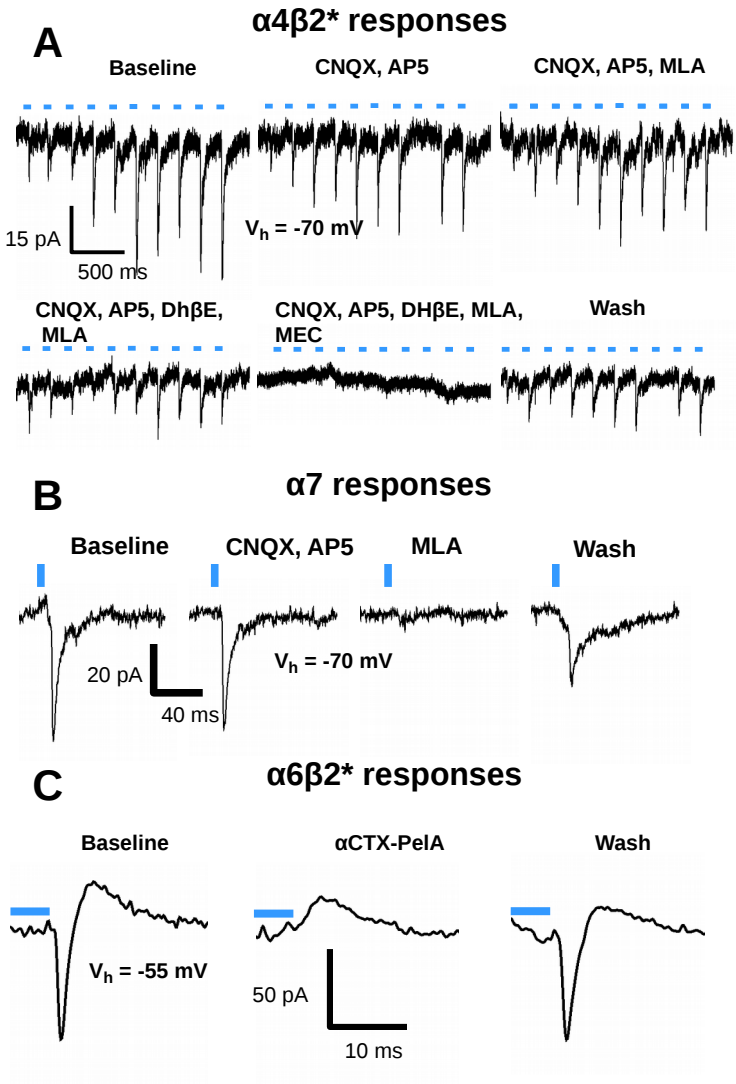

**Figure 3.6.** Blue light evoked nicotinic EPSCs mediated by stimulation of cholinergic terminal in the SNc were sensitive to subtype specific nAChR antagonists. (A) Example of evoked EPSC currents mediated mainly by DHβE sensitive α4β2* and another residual component of nAChR current that was MEC sensitive but MLA and DHβE insensitive. (B) α7 nAChR mediated responses, which were abolished by MLA. (C) The inward current of the biphasic responses was mediated by α6β2* nicotinic receptors and blocked by αCTX-PelA.

### 3.1.3 The medial SNc mediates mainly disynaptic inhibitory or monosynaptic biphasic currents produced by ACh and GABA coreleased onto DA neurons

Unlike the predominantly excitatory responses in the lateral SNc, our recordings in medial SNc DA neurons expressed largely indirect outward currents or biphasic inward and outward currents. In 52% of all medial DA SNc neurons recorded, we observed disynaptic inhibitory postsynaptic currents (IPSCs) mediated by presynaptic nAChRs (indirect IPSCs) in response to 5 ms of blue light stimulation of cholinergic terminals (Fig. 3.7 and Table 3.3). These indirect IPSCs were sensitive to both nAChR antagonist cocktail (DHβE, MLA and MEC) and gabazine (SR95531, selective for $GABA_A$) (Fig. 3.7 and Table 3.1). Plotting current against voltage at different holding potentials from -100 mv to +40 mV for a direct $GABA_A$ mediated current in the presence of nAChR antagonists indicated that the currents reversed at -82 mV, near the reversal potential for chloride ($E_{Cl}$ = -83 mV) (Fig. 3.7C,D). While in 42% of recorded DA neurons, in addition to blue light evoked nicotinic EPSCs held at -70 mV, we recorded blue light evoked IPSCs (direct monosynaptic IPSCs) from the same cells when held at -20 mV (Table 3.3). Although for the biphasic currents, the outward IPSCs were resistant to nAChR antagonists but sensitive to bicuculline ($GABA_A$ receptor antagonist) inhibition,

the inward currents were blocked by nAChR antagonists (Fig. 3.8, Table 3.3). This raised the question, how could GABAergic currents result from ACh release if not mediated by presynaptic nAChRs? We suspected that we discovered a population of cholinergic terminals in the medial SNc that in addition to releasing ACh also coreleased GABA.

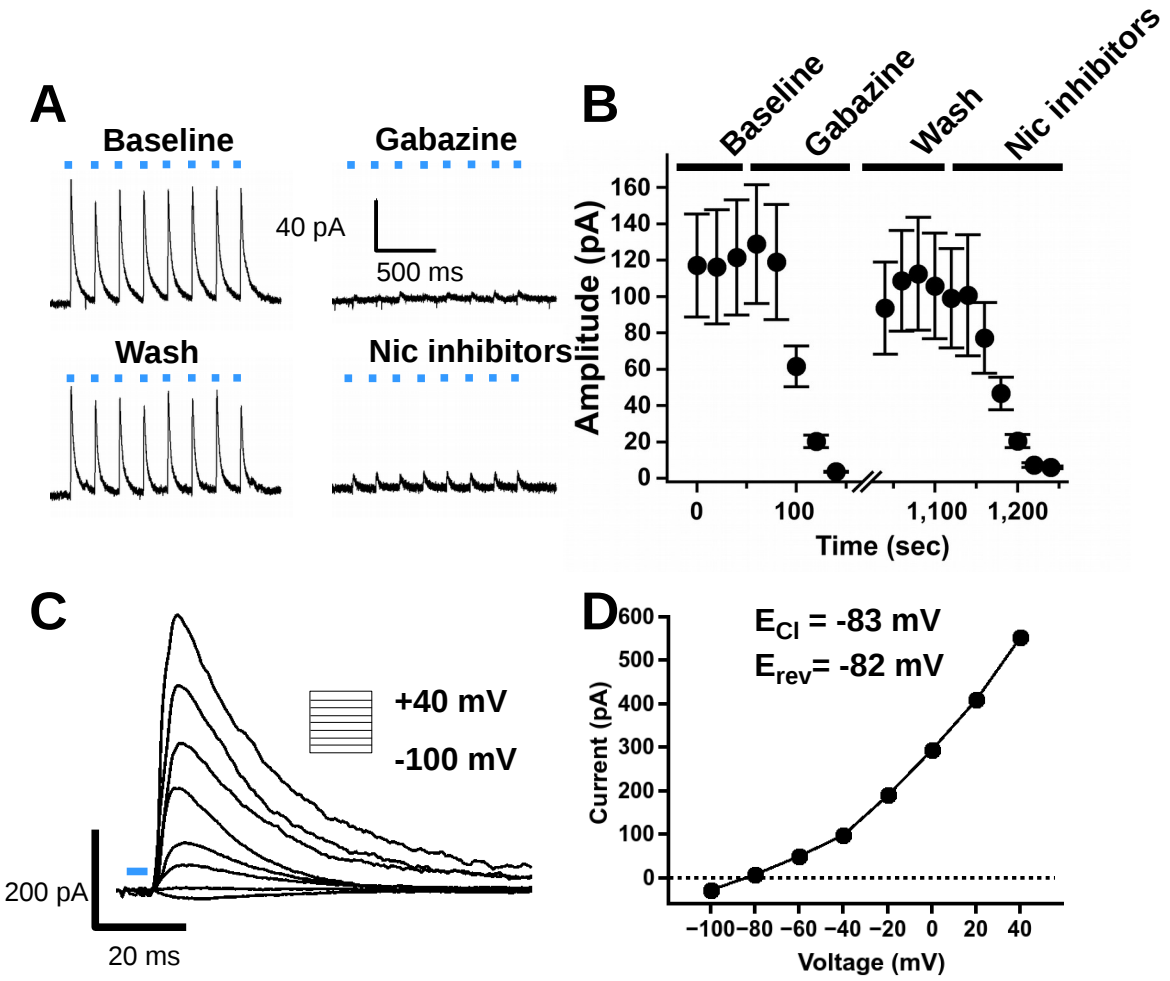


**Figure 3.7.** Medial SNc expresses mainly GABAergic mediated cholinergic neurotransmission.
(A) Traces of a voltage-clamped DA neuron in the medial SNc showing that LED blue light activation of cholinergic fibers elicits a fast IPSC mediated by presynaptic nicotinic receptors. The disynaptic (indirect) response was blocked by both $GABA_A$ receptor and nAChR antagonists. Cell is held at -20 mV. (C) An example of blue light evoked

monosynaptic (direct) GABA currents held at different potentials in the presence of nAChR antagonists, and its corresponding current-voltage plot (D).

To address whether a population of medial DA SNc neurons received coreleased ACh and GABA neurotransmission, we performed whole-cell patch-clamp recordings from brain slices obtained from ChATcre-ChR2-VGAT KO mice, in which the VGAT GABA transporter was floxed only in cholinergic neurons and compared to ChATcre-ChR2-VGAT WT mice. Our results were supportive of coreleased ACh and GABA neurotransmitters, as recordings from SNc DA neurons from ChAT-ChR2-VGAT KO mouse brain slices showed fully intact nAChR currents but significantly diminished $GABA_A$ current responses (42 ± 8 pA, n= 5 neurons) as compared to WT (263 ± 16 pA, n = 5 neurons) (Fig. 3.8C) ($t(8) = 12.4$, $p < 0.0001$, t-test). However, we did not see any difference in the amplitude of indirect $GABA_A$ currents between VGAT KO (63 ± 22 pA) and VGAT WT mice (60 ± 10 pA)(Fig. 3.8C) ($t(6) = 0.16$, $p = 0.44$).

The diminished GABAergic currents for mice with VGAT deleted solely in cholinergic neurons was one evidence supporting neurotransmitter corelease. A second line of evidence was the difference in latencies of the direct and indirect GABAergic currents. By plotting the currents latencies for both direct and indirect responses against blue LED power stimulation, we found that for direct GABAergic responses latencies were significantly less (4.6 ± 0.3 ms) than that of for indirect GABAergic currents (8.4 ± 0.4 ms) ($t(6) = 8.3$, $p < 0.0001$) and the blue light stimulation threshold of direct GABA was less than indirect GABA, suggesting that direct responses are monosynaptic, while, indirect responses are disynaptic (Fig. 3.8C). Furthermore, for biphasic GABA-nAChR

current responses showed that the direct monosynaptic GABAergic current preceded the nicotinic current, while the onset of the indirect disynaptic GABAergic current occurred following the onset of the nAChR current (Fig. 3.8D, E).

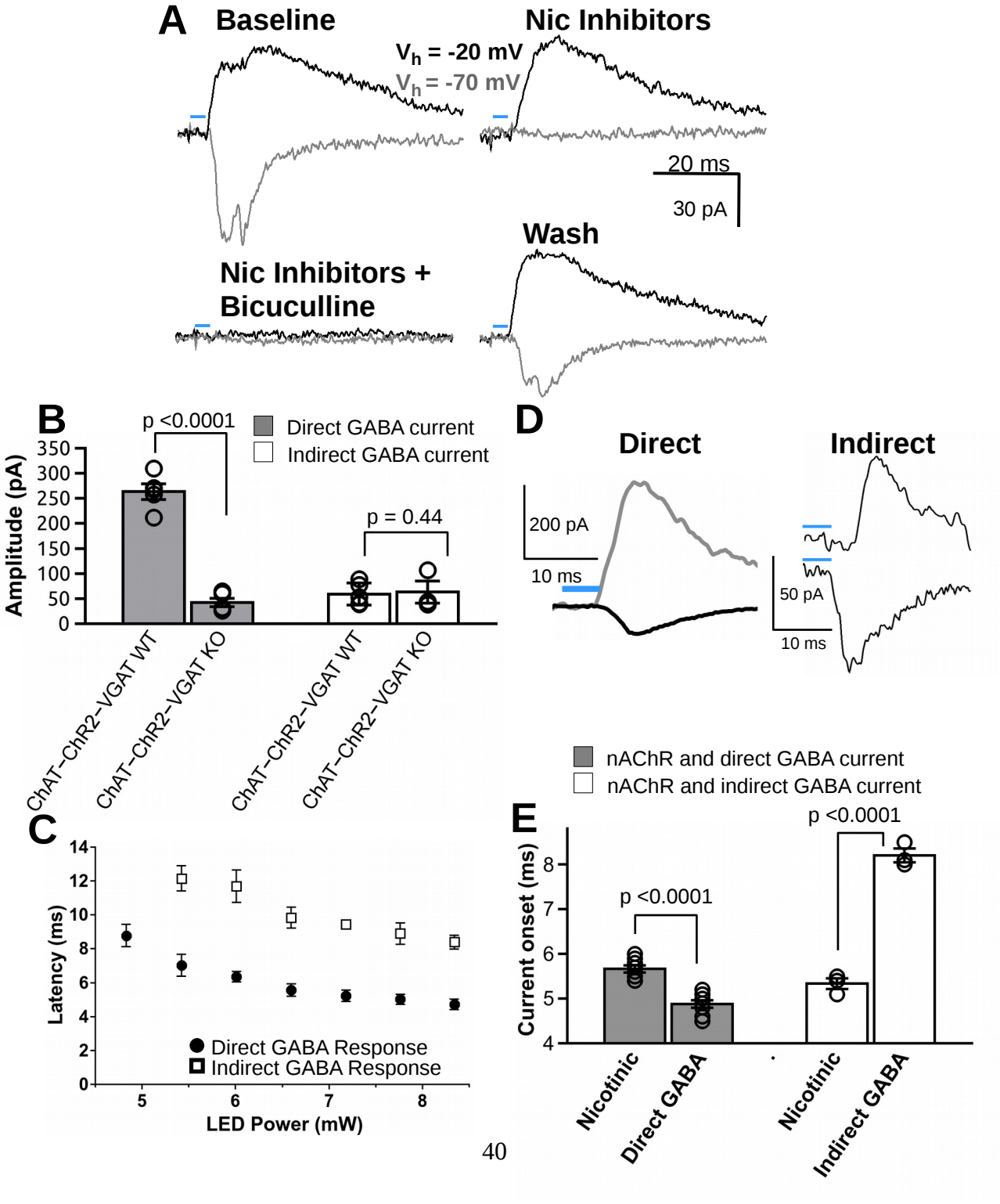

**Figure 3.8.** Corelease of ACh and GABA mediates biphasic GABAergic and nAChR currents in the medial SNc.
(A) Example traces of bicuculline sensitive monosynaptic (direct) $GABA_A$ current (Vh= -20 mV) and nAChR antagonist cocktail (MEC, MLA and DHβE) sensitive nicotinic current (Vh= -70 mV) recorded in the same DA neuron, indicating corelease of ACh and GABA with optogenetic activation of cholinergic terminals in the medial SNc. The lack of inhibition of $GABA_A$ currents with nAChR inhibitors suggest release of GABA from cholinergic neurons. (B) Graph shows that the direct monosynaptic $GABA_A$ currents are significantly reduced in ChAT-ChR2-VGAT KO mice as compared to ChAT-ChR2-VGAT WT. No differences were found in blue light evoked disynaptic (indirect) $GABA_A$ currents between ChAT-ChR2-VGAT WT and ChAT-ChR2-VGAT KO mice. (C) Onset latencies for direct and indirect IPSCs over different blue light stimulation intensities showing that indirect $GABA_A$ current responses had nearly double the onset latency than monosynaptic direct $GABA_A$ current responses. (D) Example traces of biphasic direct and indirect $GABA_A$ mediated IPSCs with their corresponding nAChR currents. (E) Summary graph indicating that the mean latency of current onset for nAChR currents is significantly greater than that of direct GABAergic currents, while the mean latency of current onset for nAChR currents is significantly less than that of indirect GABAergic currents.

Although 94% of medial DA neurons expressed cholinergic mediated GABA currents, some of which were biphasic, there were a minority of cells in the medial SNc (6%, 5 of 81 cells) that expressed purely an excitatory current, which were mostly nicotinic responses (4 of 81 cells) except for one cell containing glutamatergic responses (Table 3.3).

We further characterized the receptor subtypes conveying the evoked nicotinic responses from either medial or lateral SNc using pharmacology, and found some responses sensitive to inhibition with DHβE, suggesting α4β2* nAChRs. We also found α7 nAChRs, as these evoked nicotinic currents were inhibited by MLA, and some inward current responses that were blocked by α-conotoxin Pel-A (specific for α6β2 nAChRs) (Fig. 3.6). Interestingly, when analyzing the kinetic properties of the AMPA, α4β2* and

α7 nAChR responses held at -70 mV we observed distinct activation ($F(2,10) = 7.38$, $p = 0.01$) and deactivation kinetics ($F(2,10) = 23.4$, $p = 0.0002$) (Fig. 3.9). The disynaptic glutamatergic responses had the fastest 10-90% rise time of 0.93 ± 0.08 ms and decay tau of 2.98 ± 0.43 ms but were insignificantly different than that for α7 mediated responses, which had a rise time of 1.7 ± 0.4 ms and decay tau of 4.7 ± 1.0 ms ($p = 0.74$ and $p = 0.70$, respectively, Tukey HSD). α4β2 mediated responses had the slowest kinetics with a mean rise time of 4.7 ± 1.3 ms and decay tau of 16.4 ± 2.5 ms that were significantly slower than AMPA glutamatergic ($p = 0.01$ and $p = 0.0002$, respectively, Tukey HSD) and α7 nAChR responses ($p = 0.04$ and $p = 0.0009$, respectively, Tukey HSD) (Fig. 3.9).

Thus, in all, these results tell us that the medial SNc receives predominantly inhibitory while the lateral SNc receives mainly excitatory cholinergic mediated neurotransmission.

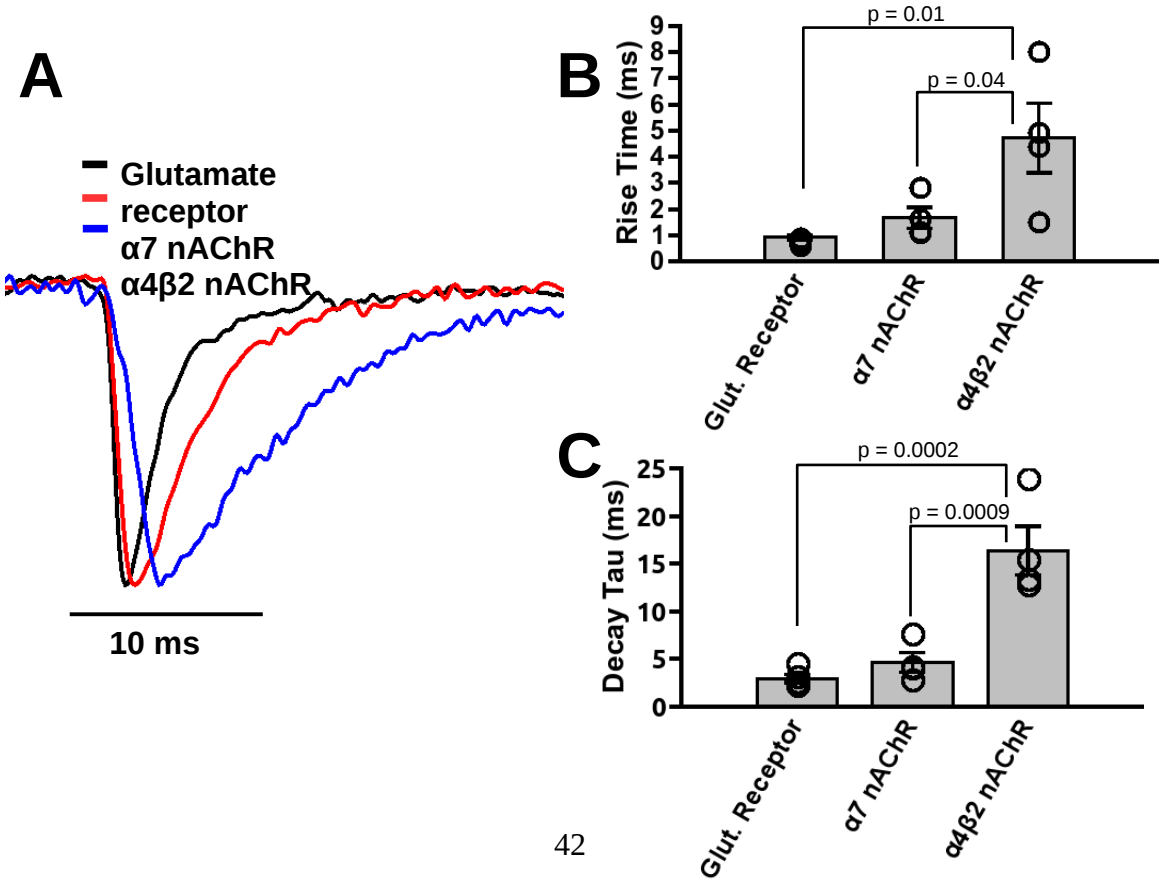

**Figure 3.9.** Comparing kinetics of evoked EPSCs mediated by cholinergic system in SNc. (A) Example traces of monosynaptic (α4β2* and α7, blue and red traces) and disynaptic (glutamatergic, black trace) responses. (B) Rise time for monosynaptic (α4β2* and α7, n=4) and disynaptic (glutamatergic, n=5). (C) Decay tau for monosynaptic (α4β2* and α7, n=4) and disynaptic (glutamatergic, n=5).

### 3.1.4 ACh and GABA colocalization in brainstem cholinergic nuclei and cholinergic terminals in SNc

As further evidence of ACh and GABA corelease, we sought to find out whether the source of cholinergic neurotransmission to the SNc, namely the PPT and LDT, comprised neuronal somata that contained both neurotransmitters ACh and GABA. We performed immunohistochemistry using an antibody against GABA on brain sections from knock-in mice (n = 3) that cre-dependently expressed tdTomato in choline acetyltransferase positive cells (ChATcre-tdTomato). Our immunohistochemistry results showed that in the PPT 57% of ChAT positive neuronal soma also expressed GABA, while in the LDT 44% of neurons positive for ChAT also expressed GABA immunostaining (Fig. 3.10).

The LDT and PPT neurons innervate a variety of brain regions in addition to the SNc. Therefore, to ensure that in the medial SNc there is colocalization of ACh and GABA containing terminals, we immunolabeled for vesicular acetycholine transporter (VAChT) and vesicular GABA transporter (VGAT) and imaged z-stacks of images with confocal microscopy. Results showed that some terminals labeled as small (~1 μm diameter) puncta for both VAChT and VGAT, indicating colocalization of ACh and GABA in individual terminals (Fig. 3.10). To ensure that this was true colocalization and not alignment of the two different labeled puncta due to chance, we performed quantitative colocalization analysis by calculating the Manders coefficients of the degree

of overlap of VAChT label to VGAT label (M1) and vice versa (M2). Then we rotated the image of one of the images 90º relative to the other and recalculated the Manders coefficients so that if there was nonspecific colocalized labeling due to chance then the Manders coefficients should not change with image rotation. Both M1 and M2 of unrotated images were significantly greater than those in which one of the images was rotated 90º, indicating that VAChT and GABA are truly colocalized in the terminals (M1 vs rotated M1: $p < 0.0001$, Wilcoxon rank sum test; M2 vs rotated M2; $p < 0.0001$, Wilcoxon rank sum test) (Fig. 3.10F).

Hence, our immunohistochemistry data supported the notion of ACh-GABA corelease onto SNc DA neurons as we confirmed that there were some cholinergic terminals in the medial SNc containing both ACh and GABA, while the potential source of these terminals, a subpopulation of neurons from the LDT and PPT also contained both neurotransmitters.

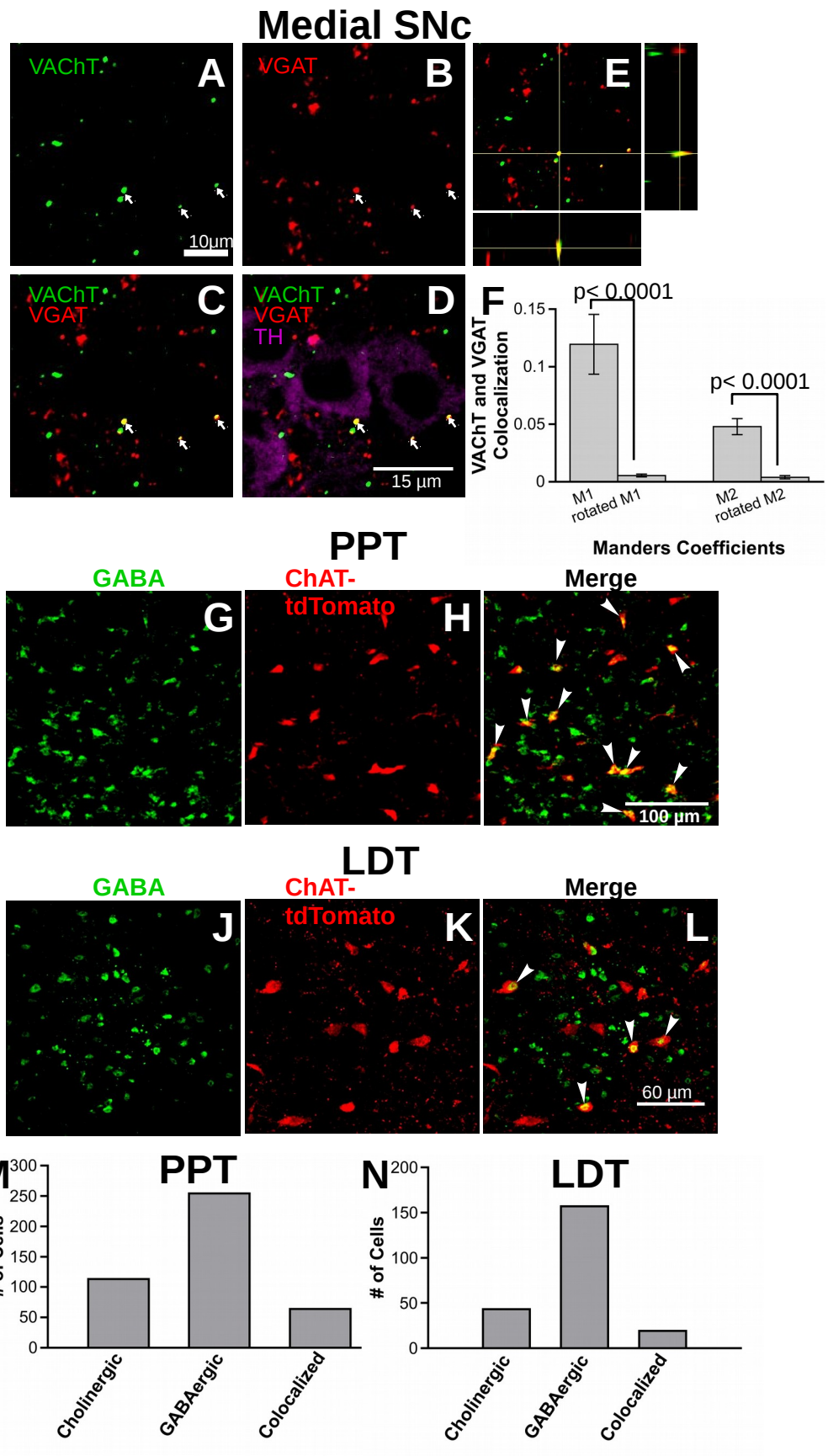
Medial SNc
VAChT
A
10µm
VGAT
B
E
VAChT
VGAT
C
VAChT
VGAT
TH
D
15 µm
F
p< 0.0001
p< 0.0001
VAChT and VGAT Colocalization
0.15
0.1
0.05
0
M1
rotated M1
M2
rotated M2
Manders Coefficients
PPT
GABA
G
ChAT-tdTomato
H
Merge
100 µm
LDT
GABA
J
ChAT-tdTomato
K
Merge
L
60 µm
M
PPT
# of Cells
300
250
200
150
100
50
0
Cholinergic
GABAergic
Colocalized
N
LDT
# of Cells
200
150
100
50
0
Cholinergic
GABAergic
Colocalized

**Figure 3.10.** Colocalization of ACh and GABA in cholinergic terminals in the medial SNc and colocalization of ACh and GABA in PPT and LDT neurons.
(A-D) Punctal immunostaining of cholinergic (VAChT) and GABAergic (VGAT) markers in presynaptic terminals in the medial SNc. DA neurons are immunolabeled against tyrosine hydroxylase (TH). (E) VAChT and VGAT colocalization is shown in the XY, XZ and YZ planes. (F) Quantitative analysis of colocalization by calculating the Manders coefficients (M1 and M2). Comparison showing that the M1 colocalization index was significantly greater than M1 when one of the two color channels of images was rotated 90 degrees relative to the other ($p < 0.0001$, Wilcoxon rank sum test); ditto for M2 ($p < 0.0001$, Wilcoxon rank sum test). (G-I) Immunohistochemistry of PPT brain slices from ChAT-tdTomato Ai9 mice showing some neuronal soma with colocalization of GABA and ChAT (arrows head). (J-L) Immunohistochemistry of LDT brain slices from ChAT-tdTomato Ai9 mice showing neurons with colocalized GABA and ChAT (arrows head). Quantitative analysis of indicating GABA and ChAT colocalization in the soma of neurons in the PPT (M) and LDT (N).

### 3.1.5 Release probabilities of ACh and GABA during corelease differ and depend on the stimulation frequency

Thus far, we have found supporting evidence of ACh and GABA corelease from cholinergic terminals synapsing onto medial SNc DA neurons. We next examined the physiological properties, namely short term synaptic plasticity, of ACh and GABA synaptic corelease when stimulating the cholinergic terminals with a 1.5 sec train of blue light stimuli at two different frequencies (5 Hz and 15 Hz). Under voltage-clamp mode, we recorded nicotinic EPSCs at -70 mV and GABAergic IPSCs at -20 mV. We found that the cholinergic synapses underwent facilitation of ACh release at 5 Hz optical stimulation, with the first response starting at -22 ± 5 pA and eventually increasing to -73 ± 19 pA (n=6), while for GABA release there was a slight facilitation in GABAergic currents at 5 Hz stimulation (from 162 ± 30 pA to 209 ± 29 pA)(Fig. 3.11A). However, at a higher stimulation frequency of 15 Hz there was a steady depression of GABAergic responses during the train (from 287 ± 62 pA to 177 ± 54 pA, n=7) (Fig. 3.11B), while

the nAChR currents displayed a similar facilitation of current at 15 Hz as it did at 5 Hz (-30 ± 9 pA to -75 ± 23 pA)(Fig. 3.11B). These results suggest that with a decline of GABAergic current at 15 Hz stimulation that there would be a tipping of the balance from inhibition to excitation during higher frequency stimulation. Furthermore, the dynamic patterns of $GABA_A$ mediated currents and nAChR mediated responses during the train stimulation suggests that in the medial SNc GABA has a high probability of release, while ACh has a low probability of release.

For biphasic indirect GABA and nAChR current responses in the medial SNc DA neurons there was facilitation for both GABAergic and nAChR currents during both 5 Hz and 15 Hz stimulation (Fig. 3.11C, D).

The pattern of ACh release in the lateral SNc was very different than in the medial SNc. In the lateral SNc there was a high probability of release for ACh at both 5 and 15 Hz (Fig. 3.12A-D). At 5 Hz stimulation, the first nAChR response in the stimulation train was robust at -43 ± 6 pA but plateaued by the second response to 50% of the first nicotinic EPSC response and remained steady thereafter in the train (Fig. 3.12A, B). At 15 Hz stimulation the first nAChR response in the train was at -65 ± 16 pA and subsequently there was an exponential decay in the nAChR current responses that settled at zero current by the eleventh response in the train (Fig. 3.12C, D).

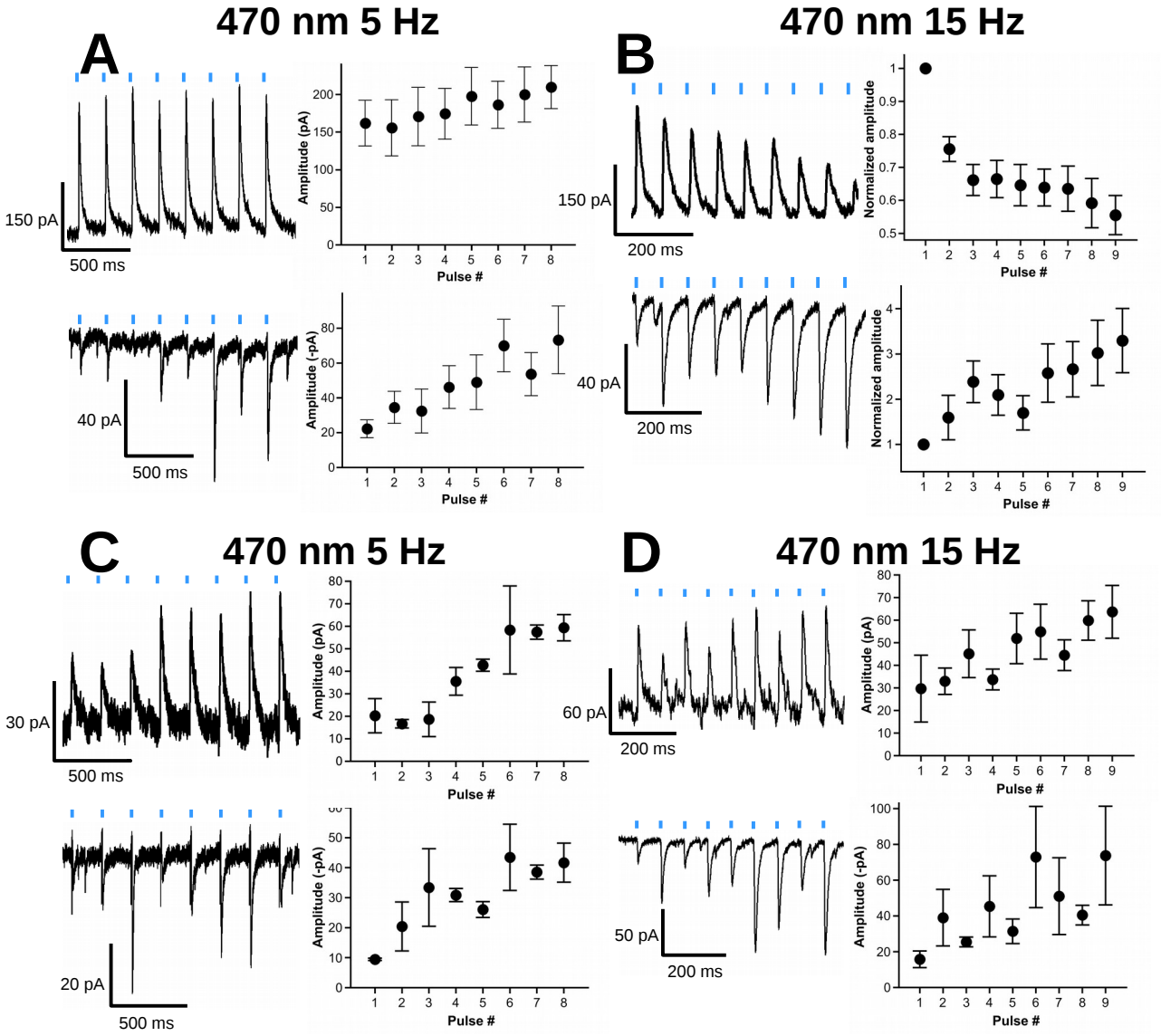


**Figure 3.11.** Frequency dependent changes in GABAergic and nAChR currents mediated by cholinergic neurotransmission in the medial SNc.

(A) Voltage-clamp recordings of medial SNc DA neurons receiving coreleased GABA and ACh showed that with repeated blue light stimulation of cholinergic terminals at 5 Hz with 5 ms pulse duration there was a robust repeatable outward GABAergic current (held at -20 mV) and a weak nAChR current (held at -70 mV), which showed facilitation with subsequent cholinergic stimulations. (B) At 15 Hz stimulation of blue light stimulation of cholinergic terminals resulted in a depression of the series of GABAergic currents, while the nAChR currents displayed current facilitation. This suggests that there is a high probability of release of GABA and a low probability of release of ACh. (C, D) For medial SNc neurons displaying indirect GABAergic and nAChR currents, both 5 Hz and 15 Hz stimulation resulted in facilitation of $GABA_A$ and nAChR currents.

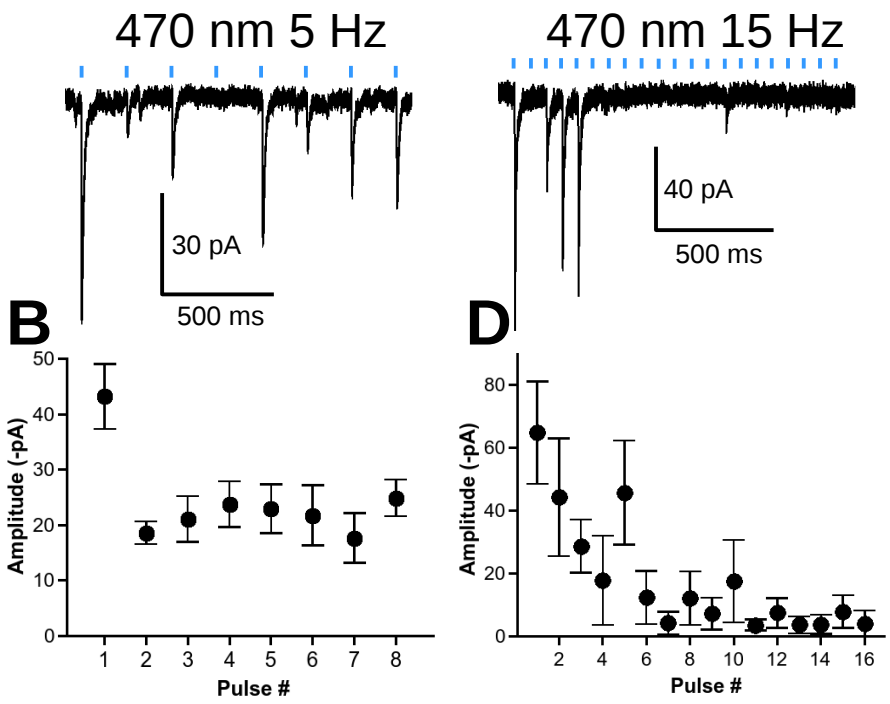


**Figure 3.12** Effects of 5 and 15 Hz blue light stimulations on evoked EPSCs in DA neurons in lateral SNc. (A) Example Voltage-clamp trace at 5 Hz stimulation. (B) Quantitative analysis showing high probability of ACh release in lateral SNc which undergoes a moderate depression at 5 Hz optical stimulation. (C) Example of a voltage-clamp trace at 15 Hz stimulation. (D) Quantitative analysis showing fast depression in the ACh mediated currents at 15 Hz optical stimulation.

### 3.1.6 ACh and GABA corelease in the medial SNc have different sensitivities to extracellular $Ca^{2+}$ concentration

We further investigated in greater detail the differential probability of release of GABA and ACh during corelease onto medial SNc DA neurons by recording both GABA and ACh mediated currents at different concentrations of extracellular $Ca^{2+}$. The hypothesis is that since ACh has a low probability of release while GABA has a high probability of release, then ACh release should be more vulnerable to being inhibited when extracellular $Ca^{2+}$ concentration is lowered than GABA release. Both cholinergic evoked GABAergic currents ($F(3,12) = 15.03$, $p = 0.0002$) and nAChR currents ($\chi^2(3) = 11.9$, $p = 0.008$) were

sensitive to lowering of extracellular $Ca^{2+}$ (Fig. 3.13A-D). GABA release was less sensitive to changes in extracellular $Ca^{2+}$ than ACh release, since there was no significant decrease in GABAergic current when extracellular $Ca^{2+}$ was dropped from 2 mM to 1.2 mM ($t(6) = 2.02$, $p = 0.18$ with Bonferoni's correction) (Fig. 3.13A, B). However, for ACh release, the nicotinic responses were completely abolished when extracellular $Ca^{2+}$ was dropped from 2 mM to 1.2 mM ($p = 0.036$, Wilcoxon signed rank test). A very low $Ca^{2+}$ (0.2 mM) caused a markable depression but not entire abolishment of the GABA current ($t(6)=5.79$, $p = 0.002$ with Bonferoni's correction), while the nAChR current was completely eliminated ($p = 0.036$, Wilcoxon signed rank test) (Fig. 3.13A-D).

Furthermore, nAChR currents had greater sensitivity to blockage of voltage-gated $Ca^{2+}$ channels than GABA currents since 150 μM $Ni^{2+}$ attenuated the nAChR current but had no effect on the GABAergic current (Fig. 3.13E, F). These results indicate that both ACh and GABA releases from cholinergic terminals in medial SNc were initiated by calcium entry through voltage-gated calcium channels. However, ACh release was more susceptible to low $Ca^{2+}$ and $Ni^{2+}$ blockade than GABA release, suggesting that ACh and GABA are released from separate vesicles from cholinergic terminals.

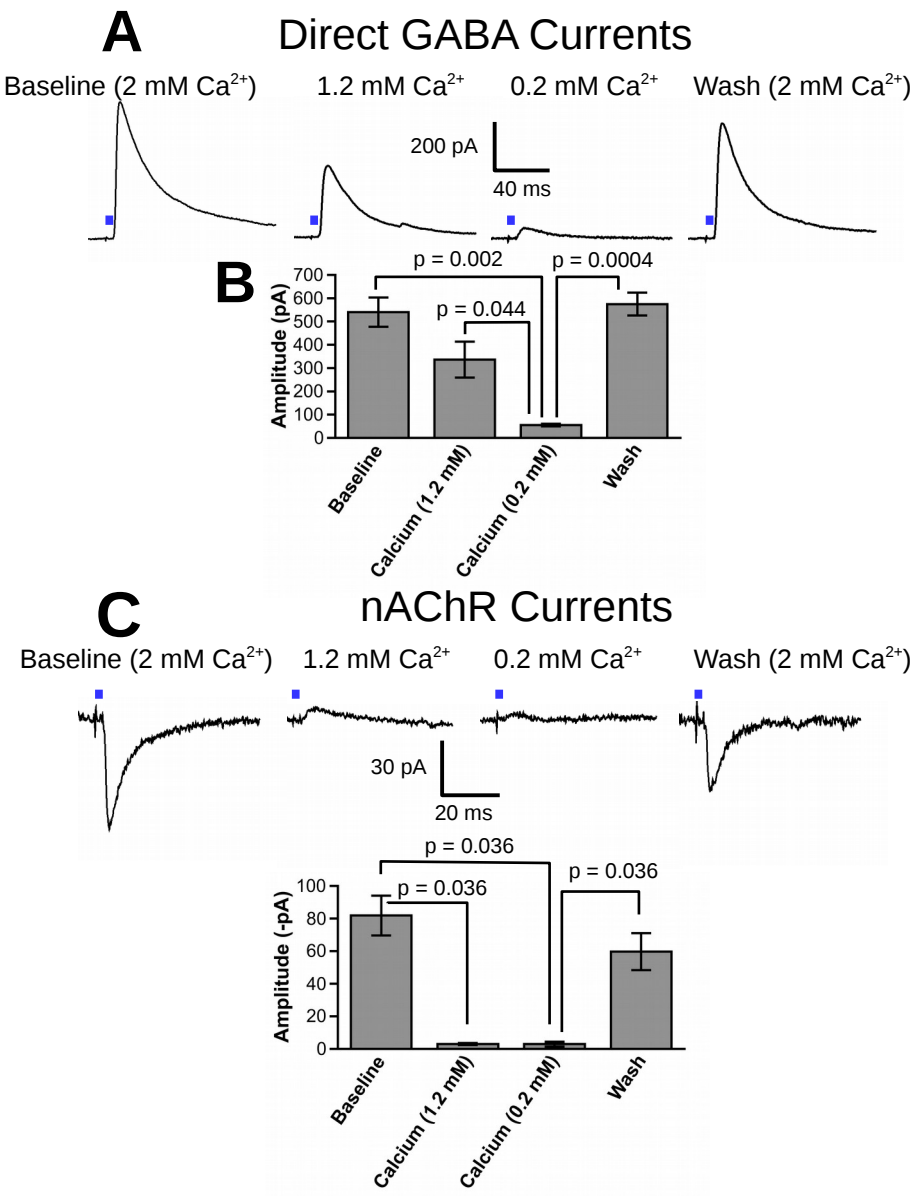
A
Direct GABA Currents
Baseline (2 mM Ca2+)
1.2 mM Ca2+
0.2 mM Ca2+
Wash (2 mM Ca2+)
200 pA
40 ms
B
p = 0.002
p = 0.0004
p = 0.044
Amplitude (pA)
700
600
500
400
300
200
100
0
Baseline
Calcium (1.2 mM)
Calcium (0.2 mM)
Wash
C
nAChR Currents
Baseline (2 mM Ca2+)
1.2 mM Ca2+
0.2 mM Ca2+
Wash (2 mM Ca2+)
30 pA
20 ms
p = 0.036
p = 0.036
p = 0.036
Amplitude (-pA)
100
80
60
40
20
0
Baseline
Calcium (1.2 mM)
Calcium (0.2 mM)
Wash
E
Direct GABA Currents
Baseline
Ni2+ (50 µM)
Ni2+ (150 µM)
Wash
200 pA
40 ms
F
nAChR Currents
Baseline
Ni2+ (50 µM)
Ni2+ (150 µM)
Wash
30 pA
20 ms

**Figure 3.13.** Coreleased GABA and ACh results in differential sensitivities of direct GABA and nAChR currents to different concentrations of extracellular $Ca^{2+}$ and $Ni^{2+}$. (A) Voltage-clamp recording traces of direct GABAergic IPSCs at 2 (baseline and wash), 1.2, and 0.2 mM extracellular $Ca^{2+}$ indicating minor sensitivity when extracellular $Ca^{2+}$ was decreased to 1.2 mM and almost completely abolished when extracellular $Ca^{2+}$ was lowered to 0.2 mM. (B) Bar graph shows that direct GABAergic current amplitude is significantly reduced only at low extracellular concentration of 0.2 mM $Ca^{2+}$. (C) Voltage-clamp traces of nAChR responses at 2 (baseline and wash), 1.2, and 0.2 mM extracellular $Ca^{2+}$. nAChR mediated responses were abolished when lowering extracellular $Ca^{2+}$ to 1.2 and 0.2 mM. (D) Bar graph shows that nAChR current amplitude was significantly abolished at both 1.2 and 0.2 mM $Ca^{2+}$. (E, F) Interestingly, the voltage $Ca^{2+}$ channel blocker $Ni^{2+}$ had no effect on the evoked GABA current at either 50 µM or 150 µM $Ni^{2+}$, but was able to completely inhibit the nAChR current at 150 µM.

### 3.1.7 DA neuronal excitability depends on frequency of stimulation and the subregions of SNc

Since our findings indicate that cholinergic neurotransmission in the lateral SNc evoked mainly excitatory currents, while in the medial SNc inhibitory or biphasic currents were prevalent, I wanted to determine how cholinergic neurotransmission would impact DA neuronal excitability in these two subregions of the SNc. I performed current-clamp recordings on DA cells when cholinergic terminals were optically stimulated at 5 and 15 Hz. For recordings in the medial SNc of DA neurons receiving coreleased ACh and GABA, optogenetic stimulation of cholinergic terminals of ChAT-ChR2 brain slices at 5 Hz, inhibited action potentials during the period of blue light LED stimulation (Fig. 3.14A-C). In contrast, cholinergic stimulation at 15 Hz caused an initial inhibition followed by a sharp increase in the firing frequency of DA neurons during blue light stimulation (Fig. 3.14D-F). To examine whether coreleased GABA was responsible for the initial inhibition of the biphasic pattern of DA excitability, we performed experiments

on brain slices from ChAT-ChR2-VGAT KO mouse brain slices and when cholinergic terminals were excited by blue light at 15 Hz there was only an increase in action potential firing and no inhibition as with the ChAT-ChR2-VGAT WT mice (Fig. 3.14I).

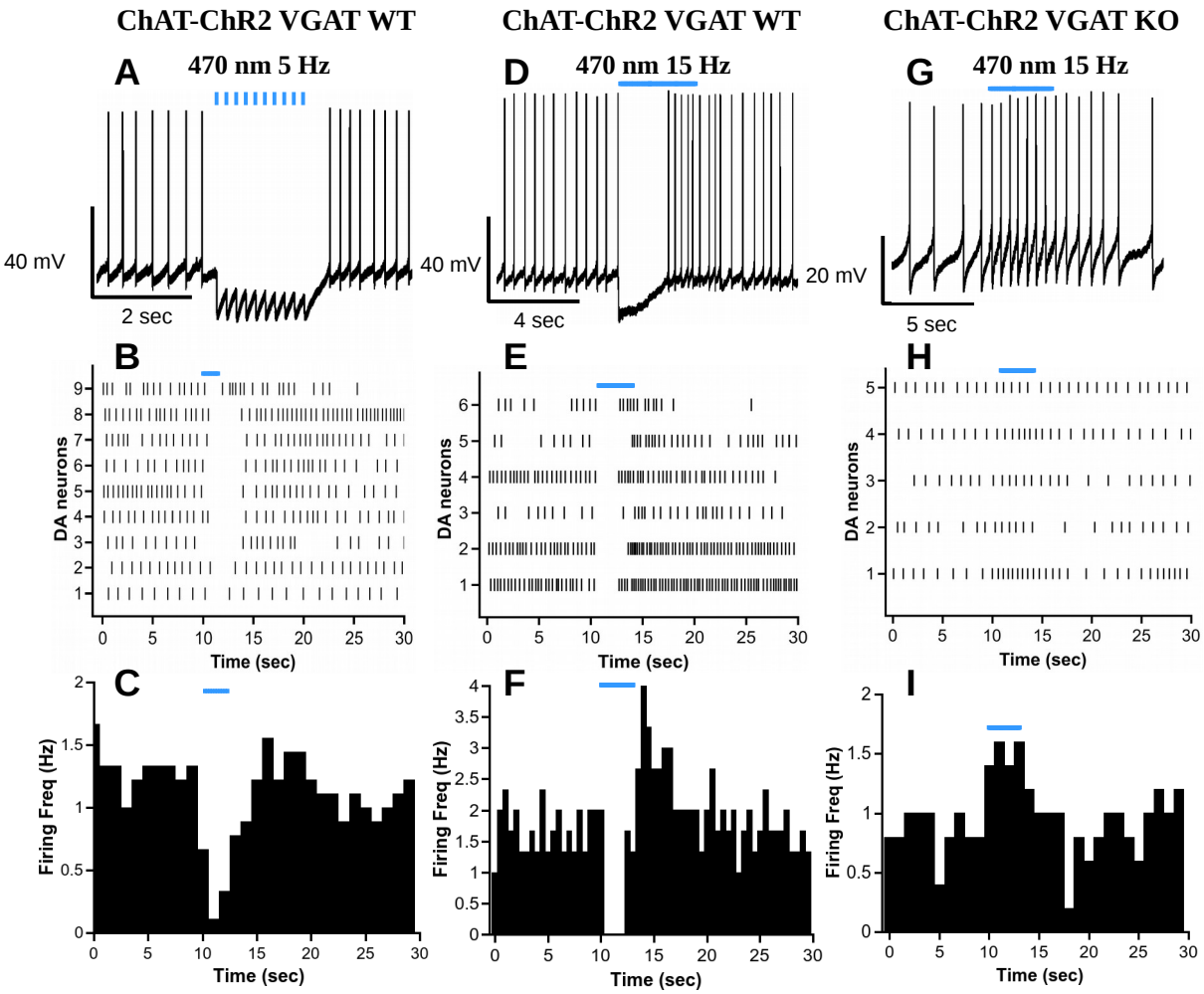


**Figure 3.14.** Frequency dependent changes in DA neuronal excitability in the medial SNc due to ACh and GABA corelease.
(A-I) Current-clamp recordings of medial SNc DA neurons with coreleased ACh and GABA. (A) Recordings from a brain section from a ChAT-ChR2-VGAT WT mouse showing an example of a current-clamp trace at 5 Hz blue LED light stimulation train (5 ms pulse duration) of cholinergic terminals, which inhibited action potential firing of the DA neuron. (B) Raster plot showing the time course of nine DA neurons with 5 Hz blue light stimulation, which produced inhibition of neuronal excitability. Each tick represents the firing of an action potential. (C) Histogram of the time course of mean firing frequency across all nine DA neurons, showing an inhibition of action potential firing

frequency during the 5 Hz train of blue light stimulation. (D) Recordings from a ChAT-ChR2-VGAT WT mouse brain section showing an example of a current-clamp trace in which DA neuronal excitability initially showed an inhibition and then an enhancement in action potential firing when the frequency of blue light stimulation was increased to 15 Hz. (E) Raster plot of six DA neurons with 15 Hz blue light stimulation. (F) Histogram of the mean firing frequency of the six DA neurons versus time at 15 Hz blue light stimulation showing initially inhibition followed by a sharp increase in firing frequency relative to baseline. (G-I) In ChAT-ChR2-VGAT KO mice there is only an increase in neuronal excitability during the blue light stimulation as shown in the current-clamp trace (G), the raster plot of five DA neurons (H) and the histogram showing the time course of the mean firing frequency of the five DA neurons (I). Together these results indicate that ACh alone increases neuronal excitability. However, when GABA is coreleased with ACh, the modulation of neuronal excitability depends on the stimulation frequency of cholinergic fibers. Lower frequency stimulation at 5 Hz only results in decreased neuronal excitability but there is a switch from inhibition to excitation during high frequency stimulation of 15 Hz.

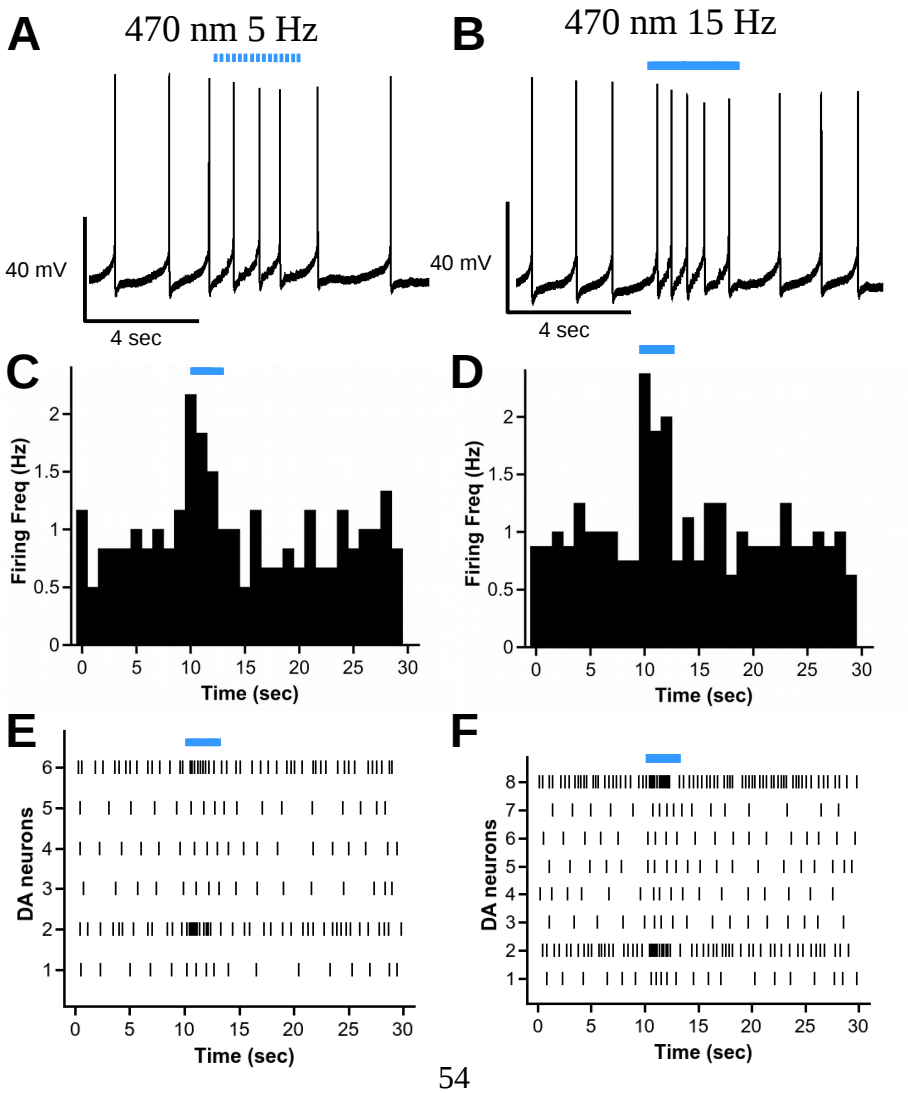

**Figure 3.15.** Frequency dependent changes in DA neuronal excitability of lateral SNc due to photostimulation of cholinergic terminals. (A-F) Current-clamp recordings of the lateral SNc DA neurons. (A) A current-clamp trace showing that 5 Hz blue light stimulation of cholinergic terminals increased firing of the DA neuron. (B) Histogram showing that the average firing frequency of six DA neurons increased with 5 Hz blue light stimulation. (C) Raster plot indicating action potential events for each of the six DA neurons with 5 Hz blue light stimulation, which increased neuronal excitability. (D) A current-clamp trace at 15 Hz stimulation showing increased firing of DA neuron. (E) Histogram time course of the mean firing frequency of eight DA neurons showing increased excitability at 15 Hz blue light stimulation. The peak excitability at 15 Hz stimulation was not significantly different than at 5 Hz ($p = 0.16$, Wilcoxon rank sum test). (F) Raster plot of action potential events of each of the eight DA neurons with 15 Hz blue light stimulation showing greater excitability.

Analysis of DA neurons firing in the lateral SNc showed that cholinergic terminal stimulation by blue light at 5 and 15 Hz augmented action potential firing during the period of stimulation (Fig. 15.3A-F). Surprisingly, we did not find any significant difference in the maximal peak of action potential firing frequency at 5 Hz ($3.4 \pm 1.5$, $n=6$) and 15 Hz ($3.9 \pm 1.4$, $n=8$) blue light stimulations ($p = 0.16$, Wilcoxon rank sum test), this is likely due to the greater depression of nAChR currents at 15 Hz (Fig. 3.12C, D) than at 5 Hz (Fig. 3.12A, B).

Thus, in general cholinergic neurotransmission in the medial SNc inhibits excitability of DA neurons, while in the lateral SNc stimulation of cholinergic transmission increases excitability of DA neurons. Furthermore, neuronal excitability can be further modulated depending on the frequency of stimulation. In particular, medial SNc neurons can switch from inhibitory to excitatory with high frequency cholinergic input.

### 3.1.8 Cholinergic neurotransmission in lateral and medial SNc differentially modulate locomotion behaviour

It is unclear the role of ACh and GABA corelease on behaviour involving the SN. To ascertain the role of GABA that is coreleased with ACh on motor function, we performed open field locomotor tests of ChATcre-ChR2-VGAT WT vs ChATcre-ChR2-VGAT KO mice. We found that in a 5 min session the ChATcre-ChR2-VGAT KO mice traveled a significantly longer distance than the ChATcre-ChR2-VGAT WT mice (Fig. 16.3B) ($t(11) = 2.24$, $p = 0.024$). Furthermore, we noticed that the ChATcre-ChR2-VGAT KO stopped less frequently to explore their surroundings, which also contributed to the longer distances traveled. To quantify this difference in exploratory behavior, we counted the number of rearings of both groups of mice and found that in 5 min open field the ChATcre-ChR2-VGAT KO had significantly lower number of rearings ($15.6 \pm 2.5$, n=7 mice) than ChATcre-ChR2-VGAT WT mice ($25.3 \pm 4.2$, n=6 mice) ($t(11) = 2.06$, $p = 0.03$).

Our electrophysiology results showed that cholinergic neurotransmission in the lateral SNc increased excitability of DA neurons, while in the medial SNc inhibited DA activity. To examine how cholinergic activity in these two subregions of the SNc affect movement, we stereotactically implanted fiber optics bilaterally into either the medial or lateral SNc (Fig. 3.16A, B) of ChATcre-ChR2 mice and optically stimulated cholinergic terminals during the open field locomotor task. The protocol used for monitoring locomotion comprised of a 5 min baseline (no optical stimulation), 5 min of discontinious photostimulation at 5 Hz, 5 min recovery (no stimulation), 5 min of discontinious

photostimulation at 15 Hz, and 5 min recovery (no stimulation) (Fig. 2.1). The 5 min periods of discontinuous photostimulation consisted of a 20 sec baseline followed by 1 min of LED train stimulation at either 5 Hz or 15 Hz with 5 ms pulse durations, 1 min no stimulation recovery, then 1 min LED stimulation at the chosen frequency with 5 ms pulse durations, then 1 min no stimulation recovery, and then ending with 40 sec photostimulation train (Fig. 2.1). Analysis of recorded videos showed that activation of cholinergic projections in the lateral SNc increased motor activity at both 5 and 15 Hz stimulations ($F(4,16) = 12.8$, $p < 0.0001$) (5 Hz vs baseline: $t(4) = 4.3$, $p = 0.012$; 15 Hz vs recovery 1: $t(4) = 5.5$, $p = 0.005$, Bonferroni's correction, n= 5 mice)(Fig. 3.17D). Interestingly, 5 Hz photostimulation of cholinergic terminals in the medial SNc significantly decreased locomotor activity ($F(4,16) = 4.08$, $p = 0.018$, $t(4) = 3.05$, $p = 0.038$, with Bonferonni's correction), whereas 15 Hz photoexcitation significantly increased locomotor activity as compared to 5 Hz stimulation ($t(4) = 3.7$, $p = 0.02$, with Bonferonni's correction) (Fig. 3.17E).

To ensure that the changes in locomotion with blue light stimulation was due to activation of ChR2 expressing cholinergic neurons and not due to potential phototoxicity, we performed negative control experiments in which blue light stimulation of fiber optics implanted in the lateral SNc were performed in α4YFP knock-in mice. These mice have the α4 nAChR subunits fused to YFP, which are highly expressed on the membranes of DA neurons (Nashmi et al., 2007) but are not activated by blue light. Our results showed that blue light stimulation at 5 or 15 Hz of the lateral SNc of α4YFP knock-in mice did not produce any changes in locomotion ($F(4,12) = 0.97$, $p = 0.46$, n=4 mice)(Fig. 3.17F).

To better show how well blue light stimulation correlated temporally to movement, we plotted the instantaneous velocity of movement for each frame analyzed and averaged over all the mice in relation to the blue light flashes used to stimulate the SNc (Fig. 3.18). In the lateral SNc optic fiber implanted ChATcre-ChR2 mice, we observed an increase in the locomotor velocity within a couple of seconds of onset of blue LED stimulation at both 5 Hz or 15 Hz and remained elevated for the 1 min duration (Fig. 3.18A, B). In contrast, for SNc medially implanted fiber optics, locomotor velocity was diminished within a few seconds of onset of 5 Hz photostimulation and remained attenuated, while at 15 Hz photostimulation a slight increase in velocity was noticible (Fig. 3.18C, D). Blue LED stimulation of the lateral SNc of α4YFP mice at 5 and 15 Hz failed to elicit any consistent pattern of effect on locomotor velocity (Fig. 3.18E, F).

Hence, cholinergic stimulation in the lateral SNc results in increased locomotion, while stimulation of cholinergic transmission of the medial SNc only at 5 Hz can decrease motor activity.

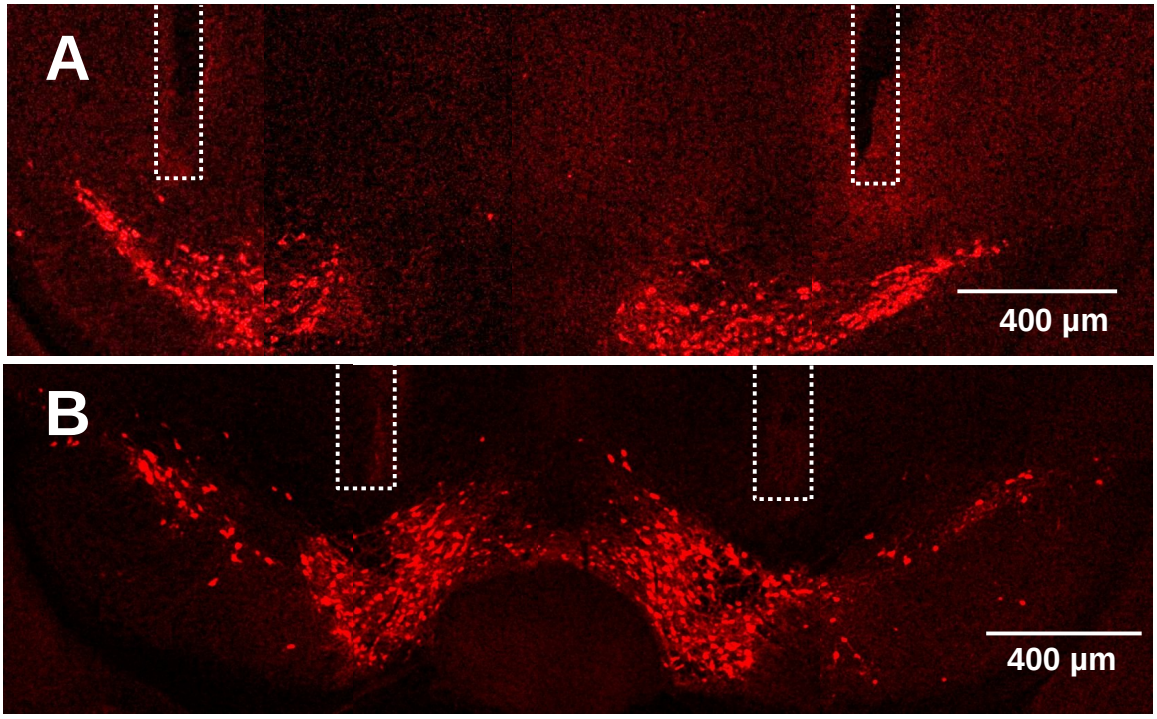


**Figure 3.16.** Coronal sections of SNc with the position of implanted optic fibers. (A) Tracks of implanted optic fibers in the lateral SNc. (B) Tracks of implanted optic fibers in the medial SNc. TH staining shown in red.

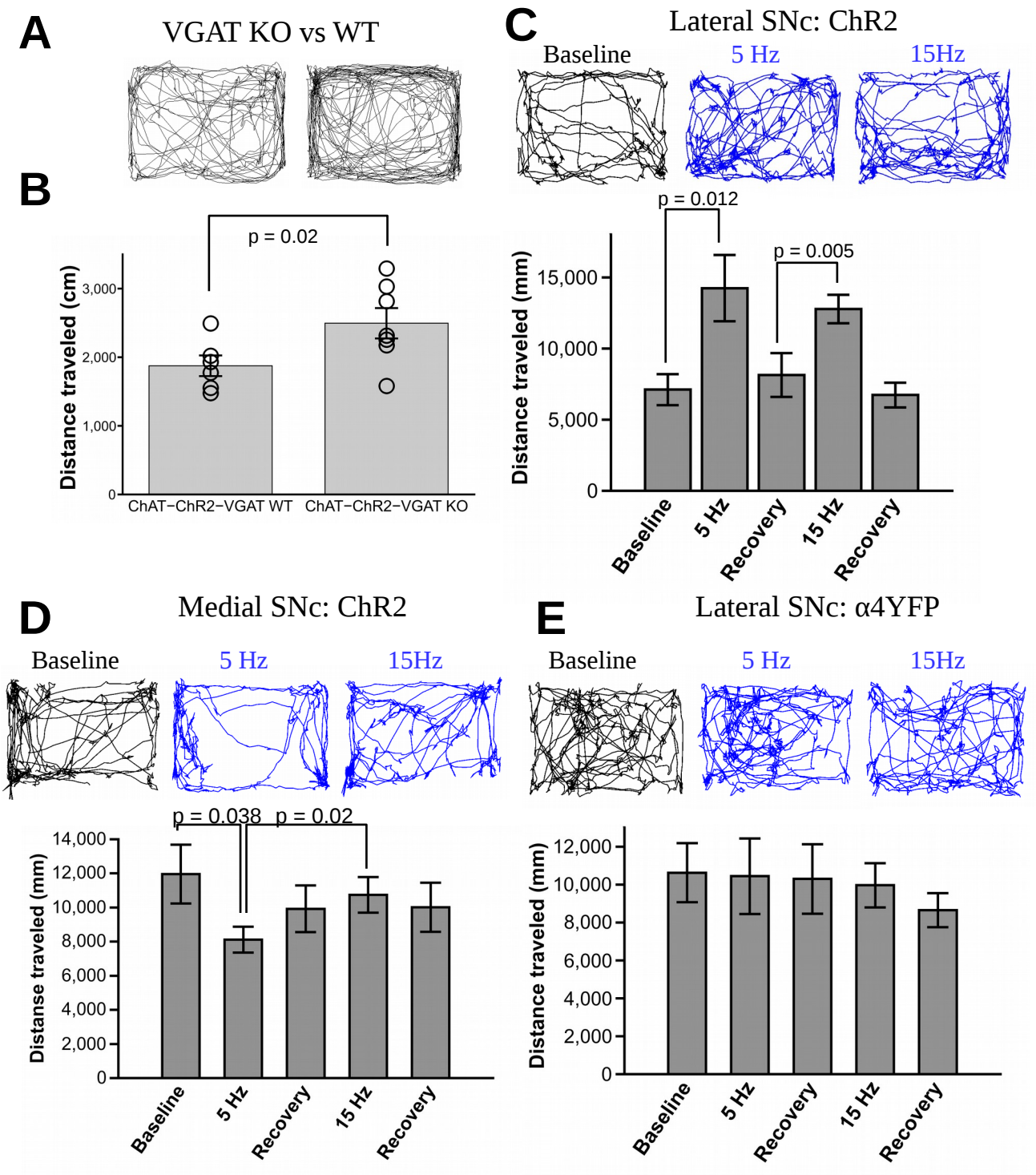


**Figure 3.17.** Optogenetic stimulation of the lateral SNc increases locomotion while stimulation of the medial SNc depresses locomotion.
(A) Representative locomotor trajectory traces in an open field arena of ChAT-ChR2-VGAT WT (WT, left) and ChAT-ChR2-VGAT KO (VGAT KO, right) mice (B) Graph showing that VGAT KO mice traveled a significantly longer distance in the open field

arena than the WT mice. (A, B) No photostimulation was employed. (C) In ChAT-ChR2 mice with fiber optics implanted into the lateral SNc the top trajectory plots show baseline activity (black trace) and activity during blue LED light stimulation at 5 Hz and 15 Hz (blue trace). Graph shows that photostimulation of lateral SNc in ChAT-ChR2 mice induced significant enhancement at 5 Hz ($p = 0.012$, paired t-test, Bonferonni's correction, n=5 mice) and 15 Hz stimulation ($p = 0.005$, paired t-test, Bonferonni's correction, n=5 mice). (D) With fiber optics implanted into the medial SNc of ChAT-ChR2 mice trajectory plots (top) and graph (below) show that photostimulation at 5 Hz decreased locomotor activity ($p = 0.038$, paired t-test, Bonferonni's correction, n=5 mice) but not at 15 Hz stimulation, which showed significantly greater locomotion than with 5 Hz ($p = 0.02$, paired t-test, Bonferonni's correction, n=5 mice). (E) As a negative control we performed optogenetic experiments on α4YFP mice, which has YFP fused to the α4 nAChR subunit, which is strongly expressed on the membranes of SNc DA neurons. Trajectory plots. and plot of the mean distance traveled showed that blue light photostimulation α4YFP mice with fiber optic implants into the lateral SNc did not significantly alter locomotion neither at 5 Hz nor at 15 Hz stimulations.

Lateral SNc (ChR2)

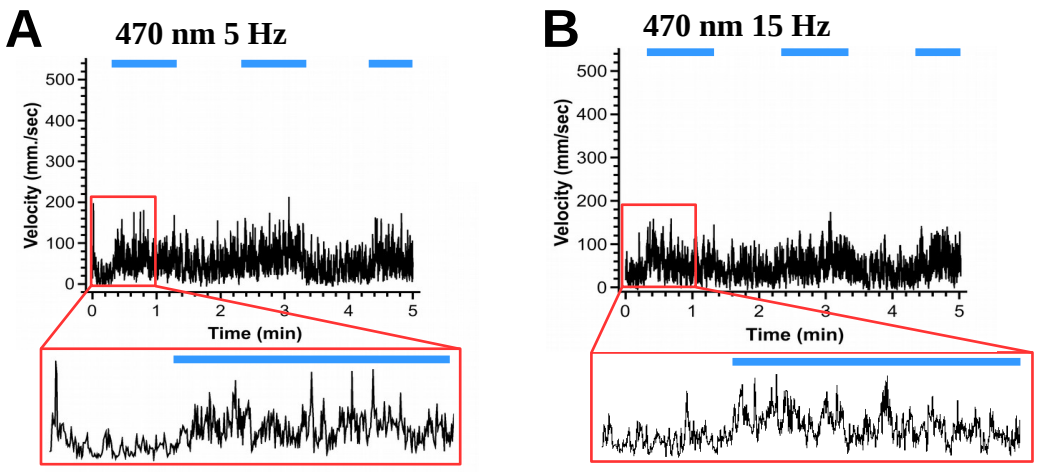


Medial SNc (ChR2)

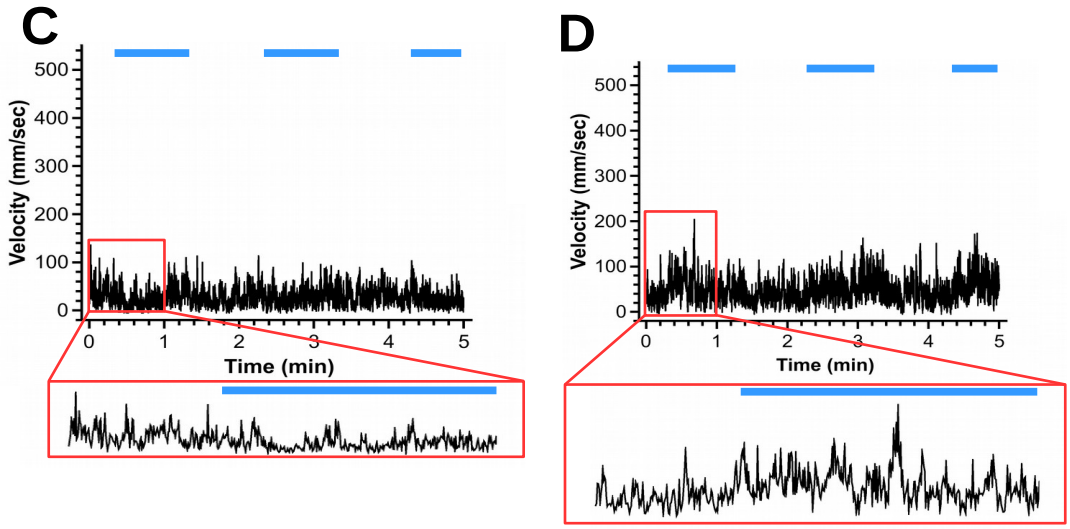


Lateral SNc (α4YFP)

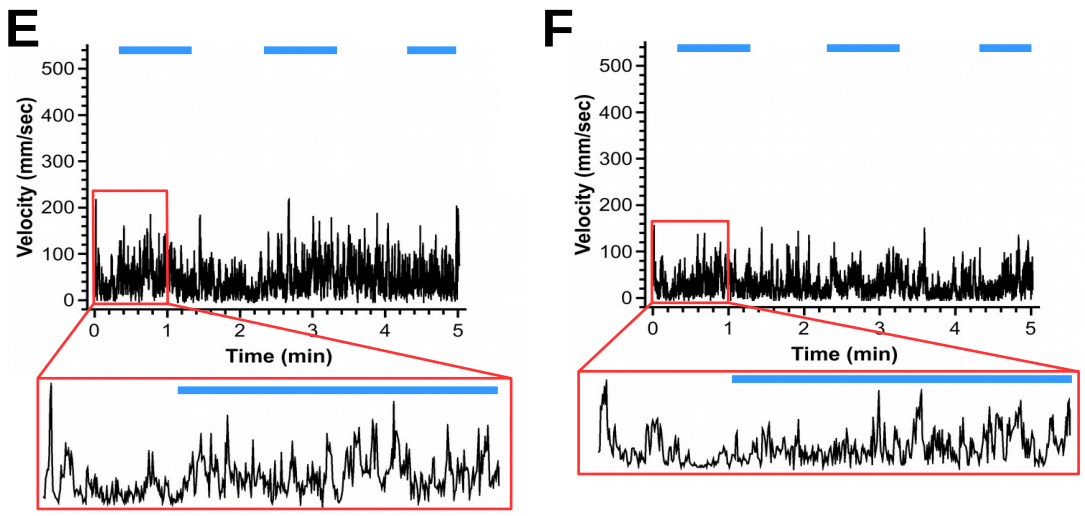

**Figure 3.18.** Velocity of mice during open field tests. (A) The graph showing the time course of locomotion velocity averaged over five ChR2 mice with optic fibers implanted in the lateral SNc during open field test. Blue bars indicate 5 Hz blue light stimulation at 5 ms pulse duration. There was an increase in locomotion velocity during blue light stimulation at 15 Hz as shown in the inset. (B) Locomotor velocity averaged for five ChR2 mice with optic fibers implanted in lateral SNc during intermittent 15 Hz blue light stimulation (blue bars). There was an increase in locomotor velocity from prestimulation to 15 Hz blue light stimulation period. (C) Average velocity of five ChR2 mice implanted with optic fibers into the medial SNc and photostimulated at 5 Hz. Inset shows that locomotor velocity decreased during 5 Hz blue light stimulation. (D) Average velocity of five ChR2 mice implanted with fiber optics into the lateral SNc during 15 Hz photostimulation showing an increase in velocity during blue light stimulation. (E, F) A negative control experiment in which average velocity of four α4YFP mice implanted with fiber optics into the lateral SNc showed no distinct pattern of locomotor changes with either blue light stimulation at either 5 Hz or 15 Hz.

## 3.2 Discussion

From recordings of knock-in mice with targeted expression of ChR2 in cholinergic neurons, we found distinct cholinergic-mediated responses in the lateral vs the medial SNc. Light-evoked ACh release onto the lateral SNc DA neurons resulted in mainly excitatory currents (direct nicotinic or indirect glutamatergic) and a gain in neuronal excitability, while medial DA neurons mainly expressed a biphasic current (direct nicotinic and GABA) or solely an indirect GABAergic response, which mainly inhibited neuronal excitability. In a subpopulation of the medial DA neurons there was evidence of coreleased ACh and GABA. For those neurons, neuronal excitability was dependent on the frequency of cholinergic stimulation, switching from inhibitory (5 Hz stimulation) to a biphasic inhibitory-excitatory response (15 Hz stimulation). Interestingly, ChR2 stimulation in awake mice showed similar trends in motor behaviour with increased locomotion upon stimulation of cholinergic terminals in the lateral SNc, while there was

decreased locomotion with cholinergic stimulation in the medial SNc at only 5 Hz. To our knowledge, this is the first study to discover coreleased neurotransmission onto DA neurons in the SNc. Also this study was the first detailed mechanistic account of how cholinergic neurotransmission in different subregions of the SNc can mediate either excitatory or inhibitory effects on DA neuronal excitability and correspondingly increase or decrease in movement.

The cholinergic nuclei that innervate the SNc, the PPT and LDT, are heterogeneous nuclei containing cholinergic, glutamatergic and GABAergic neurons (Jia et al., 2003; Wang and Morales, 2009). Much evidence in the literature point to the fact that in general stimulation of the PPT, the major site of innervation into the SN, largely excites dopaminergic neurons (Clarke et al., 1987; Xiao et al., 2016a). Certainly, I found the increase in neuronal excitability to be the case when we stimulated cholinergic terminals that expressed ChR2 in the lateral SNc. It was found that the cholinergic neurotransmission that these neurons received were mainly direct monosynaptic nicotinic EPSCs or indirect disynaptic AMPA and NMDA glutamatergic EPSCs conveyed by presynaptic α7 nAChRs (Fig. 3.5). Furthermore, our study establishes the fact that postsynaptic nAChRs do mediate fast direct nAChR mediated neurotransmission in DA neurons in the SN due to endogenous release of ACh. Certainly, with the advent of optogenetics, fast direct nAChR neurotransmission has been more commonly found in many regions of the CNS (Arroyo et al., 2012; Bennett et al., 2012). Our results demonstrate that indeed ACh containing presynaptic terminals form functional synapses with postsynaptic nAChRs. Very likely, two modes of cholinergic neurotransmission

could be involved that includes both fast direct nAChR neurotransmission in addition to diffuse volume transmission of ACh release (Descarries, 1998; Descarries et al., 1997; Xiao et al., 2016). Interestingly, ultrastructural studies using electron microscopy have shown that in the CNS there appears to be two populations of cholinergic synapses. One is a population of ACh containing presynaptic terminals that do not form synaptic junctional complexes and are believed to be involved in diffuse volume transmission, while another population of ACh containing presynaptic terminals form synaptic structures with postsynaptic sites having postsynaptic densities (Parent and Descarries, 2008). The cholinergic input is likely from PPT and LDT as witnessed from other studies using anterograde tracing and optogenetics (Clarke et al., 1987; Gould et al., 1989; Xiao et al., 2016). The glutamatergic input into the SNc is unknown but may be from the subthalamic nucleus, which was shown by others to be positively modulated by α7 nAChRs (Xiao et al., 2015). However, the glutamatergic neurons may also originate from the PPT or LDT due to their heterogeneity of neurotransmitter content.

Unlike the lateral SNc cholinergic neurotransmission, the medial SNc largely involved indirect disynaptic GABAergic neurotransmission, mediated by $GABA_A$ receptors and presynaptic nAChRs (Fig. 3.7) and biphasic responses consisting of GABA and postsynaptic nicotinic responses. The source of the GABAergic neurotransmission is likely the SNr, since we have previously shown this population of cells to be modulated by nicotinic agonists and contained α4β2* nAChRs (Nashmi et al., 2007). These indirect disynaptic GABAergic responses led to an inhibition of DA neuronal excitability of medial SNc neurons.

What is surprising about the biphasic responses is that there were two kinds, one that is comprised of monosynaptic nicotinic and disynaptic GABAergic responses, which were very rare (3 of 81 medial SNc cells), and another population of biphasic responses resulting from ACh and GABA corelease resulting in GABAergic responses that slightly precede the nAChRs responses (31 of 81 medial SNc cells). As a result, the ACh-GABA corelease leads to net inhibition of action potential firing of DA neurons with 5 Hz stimulation of cholinergic terminals in the medial SNc. However, 15 Hz cholinergic stimulation resulted in a switch from neuronal inhibition to excitation during the stimulation train. This was due to the fact that at higher frequency, GABAergic currents show depression, which was not the case at 5 Hz. While nAChR currents show facilitation at both 5 and 15 Hz; therefore, tipping the balance toward excitation at 15 Hz. These data also suggest that for corelease, GABA containing vesicles have a high probability of release, while ACh has a low probability of release. Thus, establishing the fact that during corelease ACh and GABA are released from separate vesicles. Many reasons could explain the difference in probability of release in the medial SNc including potentially that ACh containing vesicles are farther from the $Ca^{2+}$ channels in the presynaptic active zone than the GABA vesicles or that the ACh vesicles contain an isoform of synaptotagmin with lower $Ca^{2+}$ sensitivity than the isoform of synaptotagmin tethered to GABA vesicles. Although these details were not investigated, in the present study we did show that ACh release had greater $Ca^{2+}$ sensitivity as ACh release, but not GABA release, was blocked when lowering extracellular $Ca^{2+}$ from 2 mM to 1.2 mM. ACh release was also completely inhibited when applying the voltage-gated $Ca^{2+}$ channel

blocker $Ni^{2+}$ at 150 μM, which had no effect on GABA release. Interestingly, this is in contrast to ACh release in the lateral SNc, which showed a high probability of release. Hence, probability of neurotransmitter release was not necessarily specified by the identity of the neurotransmitter but the expression of molecular components involved in vesicular release in specific brain circuits. Although the origin of ACh and GABA corelease was not determined in our study, we did find using immunohistochemistry that 44% LDT neurons and 57% of PPT neurons contained both GABA and ChAT, making these nuclei likely candidates. This is in agreement with other studies showing GABA and ACh colocalization in PPT and LDT neurons (Jia et al., 2003) but in contrast to those who reported only 1% of neurons in PPT or LDT that colocalized for ChAT and glutamic acid decarboxylase (Wang and Morales, 2009).

Another interesting finding was that for coreleased ACh and GABA, in the brain slices of ChATcre-ChR2-VGAT KO mice, direct GABAergic current was not completely obliterated. There was a much reduced but significant residual GABAergic current (21% of WT). This suggests that either there are two different release mechanisms of GABA or that there may be another vesicular transporter that less efficiently loads GABA into vesicles.

To examine the functional role of ACh and GABA corelease on motor behaviour, we compared open field locomotion in mice whose ability to release GABA were only impaired in cholinergic neurons using the ChATcre-ChR2-VGAT KO mice and found that these mice walked farther distances, with very few breaks in walking and displayed less rearings to scan and explore its surroundings. So we surmised that the seemingly

paradoxical effect of GABA coreleased with ACh is to provide interruptions in motor activity to allow other behaviours such as exploratory behaviour.

The pattern of activity of cholinergic neurons or DA neurons related to movement is quite complex. Dodson and colleagues reported that most DA neurons in the SNc had a pause in activity during onset of movement (Dodson et al., 2016). While others have shown that increased SNc activity is critical for initiation and acceleration of movement (Howe and Dombeck, 2016; Jin and Costa, 2010). Similarly, for the PPT, which is the major cholinergic nucleus that innervates the SNc, there is great complexity with the correlation of PPT neuronal firing and movement with studies showing some PPT neurons increasing in activity with movement, while others a decrease in firing with movement (Matsumura et al., 1997; Norton et al., 2011). We found that the correlation of firing of cholinergic neurons with movement largely depended on the regional innervation of the SNc, medial or lateral, and the frequency of cholinergic firing. We report that activation of cholinergic terminals in the lateral SNc resulted in increased locomotion regardless of frequency of cholinergic firing (5 or 15 Hz). This is consistent with the largely cholinergic mediated excitatory nAChR responses to enhance DA firing in the lateral SNc. However, in the medial SNc we found that low frequency stimulation of cholinergic terminals at 5 Hz led to decreased locomotion, consistent with the largely cholinergic mediated disynaptic IPSCs and biphasic coreleased ACh-GABA, which attenuated SNc DA firing. Interestingly, higher frequency (15 Hz) stimulation of coreleased ACh and GABA in the medial SNc significantly enhanced locomotor activity relative to 5 Hz, consistent with the attenuation followed by enhanced action potential

firing of SNc neurons during blue light stimulation.

Overall, our results provide new insight into the role of the cholinergic system in modulating DA neurons in the SNc. The cholinergic inputs to different subregions of the SNc may regulate the excitability of the DA neurons differentially within a tight range from excitation to inhibition which may differentially control locomotor behaviour.

# Chapter 4- Summary

Understanding the basis of how DA neuronal activity in the SNc governs movements, requires an understanding of how afferent inputs of various neurotransmitter systems creates a neuronal circuit that precisely modulates DA neuronal excitability. ACh can mediate neurotransmission through postsynaptic nAChRs or mAChRs. Two brainstem cholinergic neuclei (PPT and LDT) have major projections to the SNc, despite the fact that the precise mechanisms of cholinergic modulation of DA neuronal activity remains unclear. To dissect out the modulatory roles of the cholinergic system in regulating DAergic neuronal activity in SNc and locomotion, we have employed optogenetics along with electrophysiological and behavioural approaches.

Using whole-cell recordings of DA SNc neurons we revealed a profound heterogeneity of DA neurons with regard to morphology and electrophysiological properties between medial and laterally located SNc neurons. Furthermore, we investigated whether stimulation of cholinergic terminals in these two distinct regions of the SNc – the lateral and medial portion, may mediate different cholinergic neurotransmission modalities that would differ in modulating DA neuronal excitability. By using *in vivo* optogenetics, we also investigated how cholinergic neurotransmission in the medial and lateral SNc modifies locomotor behaviour.

Using whole-cell recordings of SNc DA neurons, most neurons in medial SNc displayed simultaneous inhibitory and excitatory currents. Some of these biphasic currents were mediated by coreleased GABA and ACh. However, the cholinergic inputs in the lateral SNc were mainly excitatory. To examine how cholinergic signaling in the

medial and lateral SNc controls mouse behaviour, we used optogenetic approaches by delivering blue light through fiber optics implanted into either medial or lateral SNc and monitored mouse locomotion behaviour. Our *in vivo* results showed that activation of the cholinergic system in the medial SNc resulted in decreased locomotion, while that for lateral SNc led to increased locomotion.

Together our data support that the cholinergic system may regulate the excitability of SNc neurons within a tight range which may translate into different kinds of locomotor behaviour.

# Chapter 5- Future directions

These results have shed new light on how cholinergic neurotransmission in different subregions of the SNc modulate DA neuronal excitability and locomotor activity. Future work needs to be performed to determine whether medial and lateral SNc are innervated by separate cholinergic nuclei, the PPT or LDT, or whether they are from different subpopulations of cholinergic neurons within the same nucleus. We need to investigate in further detail whether the PPT or LDT confers selectively medial vs lateral nicotinic mediated cholinergic responses or whether either cholinergic nuclei may be selective for mediating direct monosynaptic nicotinic neurotransmission vs the disynaptic glutamatergic or GABAergic neurotransmission in the SNc. Stereotaxic bilateral injection of adeno-associated virus encoding a cre-dependent ChR2 tagged with yellow fluorescent protein (AAV-ChR2-YFP) into either the PPT or LDT of ChAT-cre mice could be a reliable way to shed light on cholinegic innervation of medial and lateral SNc. Following AAV injections, whole-cell recordings on lateral and medial SNc DA neurons need to be performed in voltage-clamp and current-clamp modes to examine the extent that the PPT or LDT mediates GABAergic, glutamatergic and nicotinic responses in the medial and lateral SNc. GABAergic neurons of the SNr contain nAChRs and profoundly inhibit DAergic excitability (Nashmi et al., 2007). Therefore, it would be vital in the future to also record from GABAergic neurons the cholinergic mediated responses from ChATcre mice with AAV-ChR2-YFP injected into the LDT or PPT. Hence, these experiments will reveal whether the LDT or PPT make preferential targets to this population of neurons. In order to have a better understanding of cholinergic innervation

of different regions of the SN, we also need to perform tract tracing studies by injecting the retrograde tracer Alexa Fluor 555 and 488 cholera toxin subunit B (CTxB) into the lateral and medial SNc, as well as the SNr in ChAT-ChR2 mice.

Furthermore, much work needs to be performed to determine the source of ACh and GABA corelease onto DA neurons in the medial SNc. Also, unresolved is whether the GABA that is coreleased with ACh in addition to slowing down and intermittently interrupting locomotion whether it is also responsible for the rearing behaviour indicative of exploratory behaviour or whether this may involve a brain region other than the SNc that also receives ACh-GABA neurotransmitter corelease. Moreover, further immuno-electron microscopy studies need to be done in order to clarify the detailed structure of the cholinergic presynaptic terminals in the medial SNc which are responsible for ACh and GABA corelease. Therefore, we can have a better understanding of spatial distribution of ACh and GABA containing vesicles in the presynaptic terminals and also whether these vesicles are located in the same terminal, mixed in the vicinity of the same active zone or not. We found that coreleased GABA had high probability of release, while coreleased ACh had low probability of release. With immuno-electron microscopy, we can quantify whether GABA have more docked vesicles in the active zone than ACh vesicles and whether docked GABA vesicles are localized more centrally to the active zone than ACh vesicles. Although my thesis has shown evidence of fast cholinergic neurotransmission mediated by nAChRs in the SNc, more work needs to be done to map out the localization of postsynaptic nAChRs in relation to docked ACh vesicles of presynaptic cholinergic terminals to better understand the true role of cholinergic

signaling – whether Ach mediates fast postsynaptic neurotransmission signaling or whether ACh is also involved in diffuse volume transmission from remote sites.

Given the *in vivo* optogenetic results, it seems necessary to have more investigations to clarify the exact role of each cholinergic nucleus in modulating locomotion. Viral expression of channelrhodopsin to stimulate cholinergic neurons or halorhodopsin to inhibit cholinergic neurons into either PPT or LDT could help delineate how these different nuclei modulate locomotion behaviour. Furthermore, we found that stimulation of the cholinergic fibers in the medial SNc inhibited locomotion, while the lateral SNc augmented locomotion. However, we do not know whether this is context dependent. For example, does the increased locomotion with lateral stimulation depend on whether the mouse is already moving or not?

Furthermore, in attempt to understand the role of GABA coreleased with ACh, we found that the ChAT-ChR2-VGAT KO mice walked further distances and had significantly less exploratory behaviour as measured by reduced rearing, than ChAT-ChR2-VGAT WT mice. It would be interesting to perform the inverse experiment in which we compare locomotion and exploratory behaviour of mice in which the vesicular ACh transporter is conditionally knocked out only in GABAergic neurons. This will give us a fuller understanding of the role of coreleased ACh and GABA in the brain and how it modifies locomotor and exploratory behaviour.

# Chapter 6- Bibliography

Alderson, H.L., Latimer, M.P., and Winn, P. (2005). Involvement of the laterodorsal tegmental nucleus in the locomotor response to repeated nicotine administration. Neurosci. Lett. *380*, 335–339.

Arroyo, S., Bennett, C., Aziz, D., Brown, S.P., and Hestrin, S. (2012). Prolonged disynaptic inhibition in the cortex mediated by slow, non-α7 nicotinic excitation of a specific subset of cortical interneurons. J. Neurosci. Off. J. Soc. Neurosci. *32*, 3859–3864.

Avale, M.E., Faure, P., Pons, S., Robledo, P., Deltheil, T., David, D.J., Gardier, A.M., Maldonado, R., Granon, S., Changeux, J.-P., et al. (2008). Interplay of β2* nicotinic receptors and dopamine pathways in the control of spontaneous locomotion. Proc. Natl. Acad. Sci. *105*, 15991–15996.

Barter, J.W., Li, S., Lu, D., Bartholomew, R.A., Rossi, M.A., Shoemaker, C.T., Salas-Meza, D., Gaidis, E., and Yin, H.H. (2015). Beyond reward prediction errors: the role of dopamine in movement kinematics. Front. Integr. Neurosci. *9*, 39.

Bennett, C., Arroyo, S., Berns, D., and Hestrin, S. (2012). Mechanisms generating dual-component nicotinic EPSCs in cortical interneurons. J. Neurosci. Off. J. Soc. Neurosci. *32*, 17287–17296.

Bensaid, M., Michel, P.P., Clark, S.D., Hirsch, E.C., and François, C. (2016). Role of pedunculopontine cholinergic neurons in the vulnerability of nigral dopaminergic neurons in Parkinson's disease. Exp. Neurol. *275*, 209–219.

Blythe, S.N., Wokosin, D., Atherton, J.F., and Bevan, M.D. (2009). Cellular Mechanisms Underlying Burst Firing in Substantia Nigra Dopamine Neurons. J. Neurosci. *29*, 15531–15541.

Borgkvist, A., Avegno, E.M., Wong, M.Y., Kheirbek, M.A., Sonders, M.S., Hen, R., and Sulzer, D. (2015). Loss of Striatonigral GABAergic Presynaptic Inhibition Enables Motor Sensitization in Parkinsonian Mice. Neuron *87*, 976–988.

Brudzynski, S.M., Wu, M., and Mogenson, G.J. (1988). Modulation of locomotor activity induced by injections of carbachol into the tegmental pedunculopontine nucleus and adjacent areas in the rat. Brain Res. *451*, 119–125.

Calabresi, P., Picconi, B., Tozzi, A., Ghiglieri, V., and Di Filippo, M. (2014). Direct and indirect pathways of basal ganglia: a critical reappraisal. Nat. Neurosci. *17*, 1022–1030.

Champtiaux, N., Gotti, C., Cordero-Erausquin, M., David, D.J., Przybylski, C., Léna, C., Clementi, F., Moretti, M., Rossi, F.M., Le Novere, N., et al. (2003). Subunit composition

of functional nicotinic receptors in dopaminergic neurons investigated with knock-out mice. J. Neurosci. *23*, 7820–7829.

Clark, S.D., Alderson, H.L., Winn, P., Latimer, M.P., Nothacker, H.-P., and Civelli, O. (2007). Fusion of diphtheria toxin and urotensin II produces a neurotoxin selective for cholinergic neurons in the rat mesopontine tegmentum. J. Neurochem. *102*, 112–120.

Clarke, P.B., Hommer, D.W., Pert, A., and Skirboll, L.R. (1987). Innervation of substantia nigra neurons by cholinergic afferents from pedunculopontine nucleus in the rat: neuroanatomical and electrophysiological evidence. Neuroscience *23*, 1011–1019.

Cornwall, J., Cooper, J.D., and Phillipson, O.T. (1990). Afferent and efferent connections of the laterodorsal tegmental nucleus in the rat. Brain Res. Bull. *25*, 271–284.

Cui, G., Jun, S.B., Jin, X., Pham, M.D., Vogel, S.S., Lovinger, D.M., and Costa, R.M. (2013). Concurrent activation of striatal direct and indirect pathways during action initiation. Nature *494*, 238–242.

Dani, J.A., and Bertrand, D. (2006). Nicotinic Acetylcholine Receptors and Nicotinic Cholinergic Mechanisms of the Central Nervous System. Annu Rev Pharmacol Toxicol.

Dani, J.A., and Bertrand, D. (2007). Nicotinic Acetylcholine Receptors and Nicotinic Cholinergic Mechanisms of the Central Nervous System. Annu. Rev. Pharmacol. Toxicol. *47*, 699–729.

Dautan, D., Huerta-Ocampo, I., Witten, I.B., Deisseroth, K., Bolam, J.P., Gerdjikov, T., and Mena-Segovia, J. (2014). A Major External Source of Cholinergic Innervation of the Striatum and Nucleus Accumbens Originates in the Brainstem. J. Neurosci. *34*, 4509–4518.

Dautan, D., Hacioğlu Bay, H., Bolam, J.P., Gerdjikov, T.V., and Mena-Segovia, J. (2016a). Extrinsic Sources of Cholinergic Innervation of the Striatal Complex: A Whole-Brain Mapping Analysis. Front. Neuroanat. *10*.

Dautan, D., Souza, A.S., Huerta-Ocampo, I., Valencia, M., Assous, M., Witten, I.B., Deisseroth, K., Tepper, J.M., Bolam, J.P., Gerdjikov, T.V., et al. (2016b). Segregated cholinergic transmission modulates dopamine neurons integrated in distinct functional circuits. Nat. Neurosci. *19*, 1025–1033.

Deniau, J.M., Mailly, P., Maurice, N., and Charpier, S. (2007). The pars reticulata of the substantia nigra: a window to basal ganglia output. In Progress in Brain Research, (Elsevier), pp. 151–172.

Descarries, L. (1998). The hypothesis of an ambient level of acetylcholine in the central nervous system. J. Physiol. Paris *92*, 215–220.

Descarries, L., Gisiger, V., and Steriade, M. (1997). Diffuse transmission by acetylcholine in the CNS. Prog. Neurobiol. *53*, 603–625.

Dodson, P.D., Dreyer, J.K., Jennings, K.A., Syed, E.C.J., Wade-Martins, R., Cragg, S.J., Bolam, J.P., and Magill, P.J. (2016a). Representation of spontaneous movement by dopaminergic neurons is cell-type selective and disrupted in parkinsonism. Proc. Natl. Acad. Sci. *113*, E2180–E2188.

Dodson, P.D., Dreyer, J.K., Jennings, K.A., Syed, E.C.J., Wade-Martins, R., Cragg, S.J., Bolam, J.P., and Magill, P.J. (2016b). Representation of spontaneous movement by dopaminergic neurons is cell-type selective and disrupted in parkinsonism. Proc. Natl. Acad. Sci. U. S. A. *113*, E2180–E2188.

Donahue, C.H., and Kreitzer, A.C. (2015). A Direct Path to Action Initiation. Neuron *88*, 240–241.

Drenan, R.M., Grady, S.R., Whiteaker, P., McClure-Begley, T., McKinney, S., Miwa, J.M., Bupp, S., Heintz, N., McIntosh, J.M., Bencherif, M., et al. (2008). In Vivo Activation of Midbrain Dopamine Neurons via Sensitized, High-Affinity α6∗ Nicotinic Acetylcholine Receptors. Neuron *60*, 123–136.

Drenan, R.M., Grady, S.R., Steele, A.D., McKinney, S., Patzlaff, N.E., McIntosh, J.M., Marks, M.J., Miwa, J.M., and Lester, H.A. (2010). Cholinergic Modulation of Locomotion and Striatal Dopamine Release Is Mediated by 6 4* Nicotinic Acetylcholine Receptors. J. Neurosci. *30*, 9877–9889.

von Engelhardt, J., Eliava, M., Meyer, A.H., Rozov, A., and Monyer, H. (2007). Functional Characterization of Intrinsic Cholinergic Interneurons in the Cortex. J. Neurosci. *27*, 5633–5642.

Exley, R., and Cragg, S.J. (2008). Presynaptic nicotinic receptors: a dynamic and diverse cholinergic filter of striatal dopamine neurotransmission. Br. J. Pharmacol. *153*, S283–S297.

Fahn, S. (2003). Description of Parkinson’s disease as a clinical syndrome. Ann. N. Y. Acad. Sci. *991*, 1–14.

Forster, G.L., and Blaha, C.D. (2003). Pedunculopontine tegmental stimulation evokes striatal dopamine efflux by activation of acetylcholine and glutamate receptors in the midbrain and pons of the rat. Eur. J. Neurosci. *17*, 751–762.

Foster, D.J., Gentry, P.R., Lizardi-Ortiz, J.E., Bridges, T.M., Wood, M.R., Niswender, C.M., Sulzer, D., Lindsley, C.W., Xiang, Z., and Conn, P.J. (2014). M5 receptor activation produces opposing physiological outcomes in dopamine neurons depending on the receptor’s location. J. Neurosci. Off. J. Soc. Neurosci. *34*, 3253–3262.

Freeze, B.S., Kravitz, A.V., Hammack, N., Berke, J.D., and Kreitzer, A.C. (2013). Control of basal ganglia output by direct and indirect pathway projection neurons. J. Neurosci. Off. J. Soc. Neurosci. *33*, 18531–18539.

Garzón, M., Vaughan, R.A., Uhl, G.R., Kuhar, M.J., and Pickel, V.M. (1999). Cholinergic axon terminals in the ventral tegmental area target a subpopulation of neurons expressing low levels of the dopamine transporter. J. Comp. Neurol. *410*, 197–210.

Gould, E., Woolf, N.J., and Butcher, L.L. (1989). Cholinergic projections to the substantia nigra from the pedunculopontine and laterodorsal tegmental nuclei. Neuroscience *28*, 611–623.

Grace, A.A., and Bunney, B.S. (1984a). The control of firing pattern in nigral dopamine neurons: burst firing. J. Neurosci. *4*, 2877–2890.

Grace, A.A., and Bunney, B.S. (1984b). The control of firing pattern in nigral dopamine neurons: single spike firing. J. Neurosci. *4*, 2866–2876.

Grace, A.A., Floresco, S.B., Goto, Y., and Lodge, D.J. (2007). Regulation of firing of dopaminergic neurons and control of goal-directed behaviors. Trends Neurosci. *30*, 220–227.

Granon, S., Faure, P., and Changeux, J.-P. (2003). Executive and social behaviors under nicotinic receptor regulation. Proc. Natl. Acad. Sci. U. S. A. *100*, 9596–9601.

Graybiel, A.M., Aosaki, T., Flaherty, A.W., and Kimura, M. (1994). The basal ganglia and adaptive motor control. Science *265*, 1826–1831.

Hendrickson, L.M., Guildford, M.J., and Tapper, A.R. (2013). Neuronal nicotinic acetylcholine receptors: common molecular substrates of nicotine and alcohol dependence. Front. Psychiatry *4*, 29.

Henny, P., Brown, M.T.C., Northrop, A., Faunes, M., Ungless, M.A., Magill, P.J., and Bolam, J.P. (2012). Structural correlates of heterogeneous in vivo activity of midbrain dopaminergic neurons. Nat. Neurosci. *15*, 613–619.

Hirsch, E.C., Graybiel, A.M., Duyckaerts, C., and Javoy-Agid, F. (1987). Neuronal loss in the pedunculopontine tegmental nucleus in Parkinson disease and in progressive supranuclear palsy. Proc. Natl. Acad. Sci. *84*, 5976–5980.

Howe, M.W., and Dombeck, D.A. (2016). Rapid signalling in distinct dopaminergic axons during locomotion and reward. Nature *535*, 505–510.

Imperato, A., Mulas, A., and Di Chiara, G. (1986). Nicotine preferentially stimulates dopamine release in the limbic system of freely moving rats. Eur. J. Pharmacol. *132*, 337–338.

Jankovic, J. (2008). Parkinson’s disease: clinical features and diagnosis. J. Neurol. Neurosurg. Psychiatry *79*, 368–376.

Jia, H.-G., Yamuy, J., Sampogna, S., Morales, F.R., and Chase, M.H. (2003a). Colocalization of gamma-aminobutyric acid and acetylcholine in neurons in the laterodorsal and pedunculopontine tegmental nuclei in the cat: a light and electron microscopic study. Brain Res. *992*, 205–219.

Jia, H.-G., Yamuy, J., Sampogna, S., Morales, F.R., and Chase, M.H. (2003b). Colocalization of gamma-aminobutyric acid and acetylcholine in neurons in the laterodorsal and pedunculopontine tegmental nuclei in the cat: a light and electron microscopic study. Brain Res. *992*, 205–219.

Jin, X., and Costa, R.M. (2010). Start/stop signals emerge in nigrostriatal circuits during sequence learning. Nature *466*, 457–462.

Kawai, H., Lazar, R., and Metherate, R. (2007). Nicotinic control of axon excitability regulates thalamocortical transmission. Nat. Neurosci. *10*, 1168–1175.

Kravitz, A.V., and Kreitzer, A.C. (2012). Striatal Mechanisms Underlying Movement, Reinforcement, and Punishment. Physiology *27*, 167–177.

Kreitzer, A.C., and Malenka, R.C. (2008). Striatal Plasticity and Basal Ganglia Circuit Function. Neuron *60*, 543–554.

Mallet, N., Ballion, B., Le Moine, C., and Gonon, F. (2006). Cortical inputs and GABA interneurons imbalance projection neurons in the striatum of parkinsonian rats. J. Neurosci. Off. J. Soc. Neurosci. *26*, 3875–3884.

Mamiya, K., Bay, K., Skinner, R.D., and Garcia-Rill, E. (2005). Induction of long-lasting depolarization in medioventral medulla neurons by cholinergic input from the pedunculopontine nucleus. J. Appl. Physiol. Bethesda Md 1985 *99*, 1127–1137.

Mansvelder, H.D., and McGehee, D.S. (2000). Long-term potentiation of excitatory inputs to brain reward areas by nicotine. Neuron *27*, 349–357.

Mansvelder, H.D., Keath, J.R., and McGehee, D.S. (2002). Synaptic mechanisms underlie nicotine-induced excitability of brain reward areas. Neuron *33*, 905–919.

Maskos, U., Molles, B.E., Pons, S., Besson, M., Guiard, B.P., Guilloux, J.-P., Evrard, A., Cazala, P., Cormier, A., Mameli-Engvall, M., et al. (2005). Nicotine reinforcement and cognition restored by targeted expression of nicotinic receptors. Nature *436*, 103–107.

Matsumura, M., Watanabe, K., and Ohye, C. (1997). Single-unit activity in the primate nucleus tegmenti pedunculopontinus related to voluntary arm movement. Neurosci. Res. *28*, 155–165.

Maurice, N., Liberge, M., Jaouen, F., Ztaou, S., Hanini, M., Camon, J., Deisseroth, K., Amalric, M., Kerkerian-Le Goff, L., and Beurrier, C. (2015). Striatal Cholinergic Interneurons Control Motor Behavior and Basal Ganglia Function in Experimental Parkinsonism. Cell Rep. *13*, 657–666.

Mena-Segovia, J., Winn, P., and Bolam, J.P. (2008). Cholinergic modulation of midbrain dopaminergic systems. Brain Res. Rev. *58*, 265–271.

Nashmi, R., Xiao, C., Deshpande, P., McKinney, S., Grady, S.R., Whiteaker, P., Huang, Q., McClure-Begley, T., Lindstrom, J.M., Labarca, C., et al. (2007a). Chronic Nicotine Cell Specifically Upregulates Functional 4* Nicotinic Receptors: Basis for Both Tolerance in Midbrain and Enhanced Long-Term Potentiation in Perforant Path. J. Neurosci. *27*, 8202–8218.

Nashmi, R., Xiao, C., Deshpande, P., McKinney, S., Grady, S.R., Whiteaker, P., Huang, Q., McClure-Begley, T., Lindstrom, J.M., Labarca, C., et al. (2007b). Chronic nicotine cell specifically upregulates functional alpha 4* nicotinic receptors: basis for both tolerance in midbrain and enhanced long-term potentiation in perforant path. J. Neurosci. Off. J. Soc. Neurosci. *27*, 8202–8218.

Nelson, A.B., Hammack, N., Yang, C.F., Shah, N.M., Seal, R.P., and Kreitzer, A.C. (2014). Striatal Cholinergic Interneurons Drive GABA Release from Dopamine Terminals. Neuron *82*, 63–70.

Norton, A.B.W., Jo, Y.S., Clark, E.W., Taylor, C.A., and Mizumori, S.J.Y. (2011). Independent neural coding of reward and movement by pedunculopontine tegmental nucleus neurons in freely navigating rats. Eur. J. Neurosci. *33*, 1885–1896.

Nys, M., Kesters, D., and Ulens, C. (2013). Structural insights into Cys-loop receptor function and ligand recognition. Biochem. Pharmacol. *86*, 1042–1053.

Oakman, S.A., Faris, P.L., Cozzari, C., and Hartman, B.K. (1999). Characterization of the extent of pontomesencephalic cholinergic neurons' projections to the thalamus: comparison with projections to midbrain dopaminergic groups. Neuroscience *94*, 529–547.

Oldenburg, I.A., and Sabatini, B.L. (2015). Antagonistic but Not Symmetric Regulation of Primary Motor Cortex by Basal Ganglia Direct and Indirect Pathways. Neuron *86*, 1174–1181.

Omelchenko, N., and Sesack, S.R. (2005). Laterodorsal tegmental projections to identified cell populations in the rat ventral tegmental area. J. Comp. Neurol. *483*, 217–235.

Parent, M., and Descarries, L. (2008). Acetylcholine innervation of the adult rat thalamus: distribution and ultrastructural features in dorsolateral geniculate, parafascicular, and

reticular thalamic nuclei. J. Comp. Neurol. *511*, 678–691.

Parikh, V., Ji, J., Decker, M.W., and Sarter, M. (2010). Prefrontal 2 Subunit-Containing and 7 Nicotinic Acetylcholine Receptors Differentially Control Glutamatergic and Cholinergic Signaling. J. Neurosci. *30*, 3518–3530.

Perez, X.A. (2015). Preclinical Evidence for a Role of the Nicotinic Cholinergic System in Parkinson's Disease. Neuropsychol. Rev. *25*, 371–383.

Perez-Lloret, S., and Barrantes, F.J. (2016). Deficits in cholinergic neurotransmission and their clinical correlates in Parkinson's disease. Npj Park. Dis. *2*, 16001.

Picciotto, M.R., Higley, M.J., and Mineur, Y.S. (2012). Acetylcholine as a Neuromodulator: Cholinergic Signaling Shapes Nervous System Function and Behavior. Neuron *76*, 116–129.

Pienaar, I.S., Elson, J.L., Racca, C., Nelson, G., Turnbull, D.M., and Morris, C.M. (2013). Mitochondrial abnormality associates with type-specific neuronal loss and cell morphology changes in the pedunculopontine nucleus in Parkinson disease. Am. J. Pathol. *183*, 1826–1840.

Pienaar, I.S., Gartside, S.E., Sharma, P., De Paola, V., Gretenkord, S., Withers, D., Elson, J.L., and Dexter, D.T. (2015). Pharmacogenetic stimulation of cholinergic pedunculopontine neurons reverses motor deficits in a rat model of Parkinson's disease. Mol. Neurodegener. *10*.

Rinne, J.O., Ma, S.Y., Lee, M.S., Collan, Y., and Röyttä, M. (2008). Loss of cholinergic neurons in the pedunculopontine nucleus in Parkinson's disease is related to disability of the patients. Parkinsonism Relat. Disord. *14*, 553–557.

Roeper, J. (2013). Dissecting the diversity of midbrain dopamine neurons. Trends Neurosci. *36*, 336–342.

Role, L.W., and Berg, D.K. (1996). Nicotinic receptors in the development and modulation of CNS synapses. Neuron *16*, 1077–1085.

Roseberry, T.K., Lee, A.M., Lalive, A.L., Wilbrecht, L., Bonci, A., and Kreitzer, A.C. (2016). Cell-Type-Specific Control of Brainstem Locomotor Circuits by Basal Ganglia. Cell *164*, 526–537.

Rothwell, J.C. (2011). THE MOTOR FUNCTIONS OF THE BASAL GANGLIA. J. Integr. Neurosci. *10*, 303–315.

Saunders, A., Oldenburg, I.A., Berezovskii, V.K., Johnson, C.A., Kingery, N.D., Elliott, H.L., Xie, T., Gerfen, C.R., and Sabatini, B.L. (2015). A direct GABAergic output from the basal ganglia to frontal cortex. Nature *521*, 85–89.

Scarnati, E., Campana, E., and Pacitti, C. (1984). Pedunculopontine-evoked excitation of substantia nigra neurons in the rat. Brain Res. *304*, 351–361.

Scarnati, E., Proia, A., Campana, E., and Pacitti, C. (1986). A microiontophoretic study on the nature of the putative synaptic neurotransmitter involved in the pedunculopontine-substantia nigra pars compacta excitatory pathway of the rat. Exp. Brain Res. *62*, 470–478.

Schäfer, M.-H., Eiden, L.E., and Weihe, E. (1998). Cholinergic neurons and terminal fields revealed by immunohistochemistry for the vesicular acetylcholine transporter. II. The peripheral nervous system. Neuroscience *84*, 361–376.

Skinner, R.D., Kinjo, N., Ishikawa, Y., Biedermann, J.A., and Garcia-Rill, E. (1990). Locomotor projections from the pedunculopontine nucleus to the medioventral medulla. Neuroreport *1*, 207–210.

Smetana, R., Juvin, L., Dubuc, R., and Alford, S. (2010). A parallel cholinergic brainstem pathway for enhancing locomotor drive. Nat. Neurosci. *13*, 731–738.

Ungless, M.A., and Grace, A.A. (2012). Are you or aren't you? Challenges associated with physiologically identifying dopamine neurons. Trends Neurosci. *35*, 422–430.

Wang, H.-L., and Morales, M. (2009a). Pedunculopontine and laterodorsal tegmental nuclei contain distinct populations of cholinergic, glutamatergic and GABAergic neurons in the rat. Eur. J. Neurosci. *29*, 340–358.

Wang, H.-L., and Morales, M. (2009b). Pedunculopontine and laterodorsal tegmental nuclei contain distinct populations of cholinergic, glutamatergic and GABAergic neurons in the rat. Eur. J. Neurosci. *29*, 340–358.

Wang, H.-L., and Morales, M. (2009c). Pedunculopontine and laterodorsal tegmental nuclei contain distinct populations of cholinergic, glutamatergic and GABAergic neurons in the rat. Eur. J. Neurosci. *29*, 340–358.

Wess, J. (2003). Novel insights into muscarinic acetylcholine receptor function using gene targeting technology. Trends Pharmacol. Sci. *24*, 414–420.

Wonnacott, S., Barik, J., Dickinson, J., and Jones, I.W. (2006). Nicotinic receptors modulate transmitter cross talk in the CNS. J. Mol. Neurosci. *30*, 137–140.

Wooltorton, J.R.A., Pidoplichko, V.I., Broide, R.S., and Dani, J.A. (2003). Differential desensitization and distribution of nicotinic acetylcholine receptor subtypes in midbrain dopamine areas. J. Neurosci. Off. J. Soc. Neurosci. *23*, 3176–3185.

Xiao, C., Nashmi, R., McKinney, S., Cai, H., McIntosh, J.M., and Lester, H.A. (2009). Chronic nicotine selectively enhances alpha4beta2* nicotinic acetylcholine receptors in

the nigrostriatal dopamine pathway. J. Neurosci. Off. J. Soc. Neurosci. *29*, 12428–12439.

Xiao, C., Miwa, J.M., Henderson, B.J., Wang, Y., Deshpande, P., McKinney, S.L., and Lester, H.A. (2015a). Nicotinic Receptor Subtype-Selective Circuit Patterns in the Subthalamic Nucleus. J. Neurosci. *35*, 3734–3746.

Xiao, C., Miwa, J.M., Henderson, B.J., Wang, Y., Deshpande, P., McKinney, S.L., and Lester, H.A. (2015b). Nicotinic receptor subtype-selective circuit patterns in the subthalamic nucleus. J. Neurosci. Off. J. Soc. Neurosci. *35*, 3734–3746.

Xiao, C., Cho, J.R., Zhou, C., Treweek, J.B., Chan, K., McKinney, S.L., Yang, B., and Gradinaru, V. (2016a). Cholinergic Mesopontine Signals Govern Locomotion and Reward through Dissociable Midbrain Pathways. Neuron *90*, 333–347.

Xiao, C., Cho, J.R., Zhou, C., Treweek, J.B., Chan, K., McKinney, S.L., Yang, B., and Gradinaru, V. (2016b). Cholinergic Mesopontine Signals Govern Locomotion and Reward through Dissociable Midbrain Pathways. Neuron *90*, 333–347.

Zhou, F.-M., Wilson, C., and Dani, J.A. (2003). Muscarinic and Nicotinic Cholinergic Mechanisms in the Mesostriatal Dopamine Systems. The Neuroscientist *9*, 23–36.